Department of Precision and Microsystems Engineering

Slender compliant mechanism with a low axial-bending stiffness ratio for use in an exoskeleton

Stijn Houweling

Report no	: 2022.047
Coach	: Ali Amoozandeh
Professor	: Just Herder
Specialisation	: MSD
Type of report	: Master Thesis
Date	: September 16, 2022

TU Delft Delft University of Technology

Challenge the future

Slender compliant mechanism with a low axial-bending stiffness ratio for use in an exoskeleton

by

Stijn Houweling

to obtain the degree of Master of Science
at the Delft University of Technology,
to be defended publicly on Friday September 16, 2022 at 09:00 AM.

Student number:	4365518	
Project duration:	September, 2021 – September, 2022	
Thesis committee:	Prof. dr. ir. J. L. Herder,	TU Delft, chair
	Ir. A. Amoozandeh Nobaveh,	TU Delft, daily supervisor
	Dr. ir. G. Radaelli,	TU Delft, supervisor

An electronic version of this thesis is available at `http://repository.tudelft.nl/`.

TU Delft

Preface

After a couple of years I can proudly say that I finished my thesis project and my student life. It has been an amazing time at the TU Delft were I made friends and had wonderful experiences. To get to this point I had help from people along the way and would like to thank them.

First of all, thank you Ali for the meetings and effort you put into my project. You were always available and the communication was easy and friendly. Secondly, I want to thank the other members of the shellskeleton group, of which the bi-weekly meetings were always insightful and helpful. Even outside these meetings, everyone involved was available for help and it made the work easier, as it felt like we were in it together.

And lastly, I want to thank my family, friends, and girlfriend. Especially my girlfriend Anna helped me during my studies, always motivating and supporting me when I had a tough time. She is also a kind of co-author of this report as she helped with the language and the illustrations. My family always supported me and made sure I was welcome back at home, and my friends made sure to help me relax and get my mind of the study.

Stijn Houweling
Delft, September 2022

Contents

1 Introduction

The type of labor in the current market consists of many types of jobs, from desk jobs to construction. The more physically demanding, like construction or warehouse work, have one problem in common: Long-term injuries. Workers have to lift and bend all day, which puts a lot of strain on the upper and lower back and causes these injuries. This is a problem for both the employer and the employee, as the employer loses a valuable asset and the employee can lose his ability to work. One way to alleviate these problems is by using an exoskeleton, in particular a wearable back support.

Exoskeletons are defined as external support for the body. In recent years exoskeletons have been developed to assist in daily life [6]. Exoskeletons have either passive or active assistance. Active assistance is provided by an actuator that requires an external energy source. Passive assistance methods do not require any external energy source and use for example material compliance to store the energy of the user. For a wearable back support, this can be compared to a torsion spring where the spring is unloaded in the upright position and will store the potential energy of the user when the user bends. When the user stands up again, the energy will be released and assist the user in standing up. This will reduce the load on the lower back and reduces injuries in the long term. Passive exoskeletons are interesting for labor purposes because without the need for an actuator the exoskeleton will be lighter and more comfortable for the user.

A problem arising in passive back exoskeletons is the elongation of the spine. When a person bends down the skin along the spine can elongate up to 70 mm when using a stooped way of lifting 15 kg [3]. Current exoskeletons use mechanisms to account for this elongation. The most common mechanism to use is a slider on the back of the user, for example Spexor [4] and VT-Lowe[1], as seen in figure 1.1a and 1.1b. What can be seen is that the sliders are bulky, heavy, and could be uncomfortable for the user as they consist of solid rigid parts close to the skin. Another exoskeleton, the Laevo Flex, uses a mechanism to account for the elongation of the back, as seen in figure 1.1c. This mechanism has a lot of moving parts and uses multiple joints, which are expensive to produce. A solution to the elongation problem without the bulky moving parts could be to use a compliant mechanism.

Compliant mechanisms are mechanisms that use elastic deformation to achieve force and motion transmission [2]. Using a compliant mechanism can have several advantages. One advantage is that complexity of the mechanism can be greatly reduced by integrating functionality. By using the integrated functionality, the system can be much lighter than a conventional mechanism. This is important for exoskeletons, as they have to be carried by the user and thus should be as light as possible. Another advantage of using compliant mechanisms in exoskeletons is that there are fewer joints and moving parts, which reduces the risk of injury to the user and reduces the production cost, as in general, joints are more expensive than monolithic compliant parts.

A fully compliant exoskeleton can remove the joints and bulky mechanisms altogether. This is a long-term project of the shellskeleton group of the TU Delft, of which the author of this report is part. To achieve this, the group works together with Laevo to make their exoskeleton fully compliant. An earlier project, made by Robin Mak, involves a curved compliant differential mechanism with neutral stability, as can be seen in figure 1.2 [7]. It solves the moving reference issue of passive exoskeletons due to walking by introducing a differential that couples leg motions and makes a stationary reference to connect to the upper body. The location of the stationary reference is at the lower part of the spine. This report and research aim to continue improving the compliant exoskeleton and focus on the connection between the differential mechanism and the vest worn by the user.

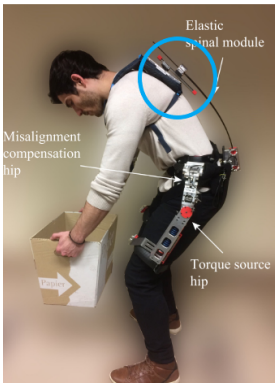

(a) The Spexor exoskeleton, with the slider encircled in blue [4]

(b) The VT-Lowe exoskeleton with a large slider on the back [1]

(c) The Laevo Flex, with the mechanism to account for the elongation encircled in blue. [5]

Figure 1.1: Three examples of current exoskeletons with sliders or some other mechanism (Laevo)

(a) Laevo exoskeleton with the differential mechanism by Robin Mak integrated, encircled in blue. The spine mechanism will be put in place of the bar that goes to the vest. [7]

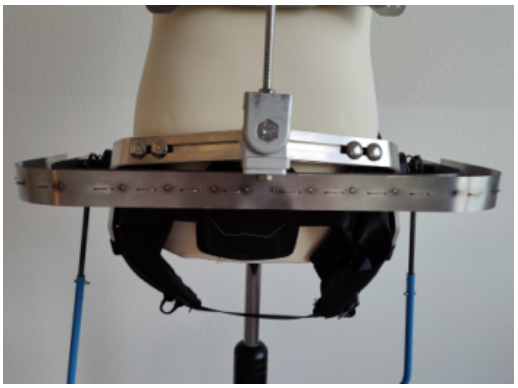

(b) Differential mechanism made by Robin Mak [7]

Figure 1.2: Design of Robin Mak

As mentioned before, the spine elongates when bending. The current design of Robin Mak does not account for this elongation. To improve the current exoskeleton, it is vital to incorporate some mechanism that can extend, while maintaining enough bending stiffness to support the bending and store energy. This can be reformulated as a mechanism with a low axial-bending stiffness ratio. The goal of this project is thus to create a slender compliant mechanism with a low axial-bending stiffness ratio suitable for use in an exoskeleton. This design should be suitable to use in combination with the design made by Robin Mak.

The biggest challenge for this project will be to account for the extension of the spine while maintaining suitable bending stiffness. This is not normal behavior for a beam. The stiffness ratio in most beams is a factor of 200 to 300, while this project aims for a ratio below 10. Other (for now less important) challenges include the curvature of the mechanism and the range of motion achieved by both the differential mechanism and the spine.

To solve these challenges several steps will be taken. The steps are listed below.

1. Design a mechanism with a low axial-bending stiffness ratio
2. Create Pseudo Rigid Body Model (PRBM)-based model to calculate the bending and axial stiffness of the mechanism
3. Create a dimensional optimization algorithm
4. Analyze the model and the mechanism by using an experimental setup

5. Create a physical wearable exoskeleton prototype to be attached to the differential mechanism

The PRBM-based model will improve the speed of the calculation of the stiffness ratio with respect to the conventional Finite Element Method (FEM). This can then be used with dimensional optimization which speeds up the overall design process. After a suitable design is made and optimized, it will be produced in a prototype and tested. Finally, a wearable exoskeleton will be made with the compliant spine incorporated.

In this report, first, a literature review will be presented in chapter 2, which will encompass a review of different mechanisms with a possible low axial-bending stiffness ratio. In chapter 3 a paper will be presented with all the findings of the research. After the paper, chapter 4 will discuss the design case for the exoskeleton from Laevo. The wrap-up will be done in the discussion in chapter 5 and the conclusion in chapter 6. Additional information can be found in the appendices, where the concept generation and stress results will be discussed. The MATLAB code for the PRBM model and the optimization can be found there as well.

2

Review paper

Review of slender mechanisms with low axial-bending stiffness ratio

Stijn Houweling
Delft University of Technology
Department of Precision Mechanism Design

***Abstract*— Slender mechanisms can be used in a multitude of applications, such as exoskeletons. In some of these applications, the need arises for a high bending stiffness coupled with low axial stiffness. While research has been done on extendable mechanisms, none took the bending stiffness into account. This literature review introduces the axial-bending stiffness ratio to look for mechanisms with this characteristic, with a focus on compliant mechanisms. The study has reviewed, classified and rated several designs that could be used as a slender mechanism with a low axial-bending stiffness ratio. The classification is done on the part of the mechanism that provides the low axial-bending stiffness, although some could be part of multiple classes. The rating system is based on the most useful performance criteria for slender mechanisms with low axial-bending stiffness and shows the advantages and disadvantages of the mechanisms and classes. It was found that metamaterials and contact-aided mechanisms show the most promise for further research.**

I. Introduction

Passive back exoskeletons can be used to prevent injuries for workers [6]. A few designs for back exoskeletons use a slider to account for the elongation of the surface of the spine [26], [14] [8]. This could lead to some discomfort for the user as the slider is an extra hindrance on the back which could prevent bending in some places. This leads to the need for a slender mechanism with a low axial-bending stiffness ratio.

A low axial-bending stiffness ratio can be compared to an extendable mechanism with relative high bending stiffness. This can either be achieved via low axial stiffness or through a motion induced by for example bending. Slender extendable mechanisms are used in a wide variety of applications, for example in the space industry [18] [15], surgical applications [11] and others [5]. Most of these papers are looking into deployable mechanisms. This will of course also extend, but most of the time requires some form of actuation. What is missing is a slender extendable mechanism that also has a high bending stiffness.

The problem presented can be explained by the beam theory. The equation for bending stiffness of a beam clamped at one end is according to the beam theory:

$$K_e = \frac{3EI}{L^3} \tag{1}$$

The equation for axial stiffness is:

$$K_e = \frac{EA}{L} \tag{2}$$

For relatively long and slender beams the bending stiffness will be much smaller than the axial stiffness. For a beam with a length of 1 m and a square cross-section with 1 cm sides, the difference is a factor of 400. This means that to lower that ratio another solution has to be found in the literature.

This paper aims to provide an overview of a slender mechanism with a low axial-bending ratio. Additionally, the mechanisms are judged on their suitability for use as a beam-like structure with non-linear bending stiffness. The focus is on compliant mechanisms, as they can have a lower weight and less wear than conventional mechanisms [7].

In Section II, first an overview will be given of the search terms used and how to replicate them. Next, the different classes will be discussed and finally the performance criteria that will be used. In Section III, all the different mechanisms found will be discussed and judged according to the criteria.

Section IV discusses the results found and Section V concludes the whole literature review.

II. Method

This section will explain how the literature is retrieved in II-A, the classification in II-B and the performance criteria in II-C

A. Literature search

To find the relevant literature a matrix has been used to make the search systematic and thorough, see table I. The columns represent all the terms used in combination with OR. The rows represent the combinations possible with AND. Not all the terms are used separately, rather multiple combinations are made to get the best results. The databases used are Scopus, Google Scholar and Web of Science.

TABLE I

Literature search terms

	AND			
	Compliant	Beam	Extendable	Bending stiffness
	Contact aided	Structure	Elongation	Deflection
	Meta-Material	Mechanism	Axial stiffness	Anisotropic
OR	Origami	Shell	Compression	
	Granular Jamming	Spine	Telescope	
	Deployable	Spline	Extension	
	Scissor	Exoskeleton		

B. Classification

During the search, a couple of main labels kept coming up. These labels are interchangeable and sometimes a mechanism can belong to multiple labels. The label it falls under is then the part of the mechanism that is most used for the ability to extend but be stiff in bending. By using a classification a better understanding of promising fields is achieved. Two mechanisms were not compatible with any of the labels. They have been put under the label other. The following labels have been defined:

1) Metamaterials: Mechanical metamaterials are man-made structures with counter-intuitive mechanical properties that originate in the geometry of their unit cell instead of the properties of each component [29]. In this case to increase the axial flexibility, while maintaining or even increasing the bending stiffness.

2) Contact aided compliant mechanisms (CA): Contact aided compliant mechanisms are a special case of compliant mechanisms. They consist of multiple elements connected by flexures that can bend. The elements are designed in such a way that they allow movement in one direction due to the flexures, but after a certain threshold is passed the stiffness jumps to the stiffness of the elements making contact. [12]

3) Origami: Origami is the art of folding paper to create aesthetic pieces without markings or cuts [10]. In modern times, origami has multiple engineering applications. Origami can alter the properties of a sheet for example, such that it can extend or twist. This is almost the same as a metamaterial, with the distinction being the fact that origami makes use of the creases [25] [16].

4) Granular Jamming: Granular materials consist of macroscopic grains interacting via contact forces. The grains are enclosed by a soft flexible material. With a trigger mechanism, usually a vacuum, the mechanism can be activated. If the mechanism is activated the grains lock each other because the vacuum pulls the enclosing material together. This will cause the stiffness of the mechanism to jump to a much higher stiffness than in the non activated state. [3] [20] [30]

C. Performance criteria

The performance criteria are selected to give an overview of the best performing slender low axial-bending stiffness ratio mechanisms. The grading system chosen is relative for all criteria except the stiffness ratio, mainly for two reasons. First, the mechanisms found all have completely different applications and scales, which makes comparing these with exact numbers of no importance. Secondly, most of the papers found do not focus on the bending and/or extending aspects. They are selected because it can be assumed that they have these properties. Thus the grading is based on comparing the mechanisms with each other. Each score will consist of a range between ++ and - - with 0 in the middle. The following criteria are selected:

Stiffness ratio This criterion is the ratio between the axial and bending stiffness. As mentioned in the introduction, the axial-bending stiffness ratio of a regular 1 m beam with a 1x1 cm

square cross-section is 400. For this criteria, the following scale is selected:

- + +: <100
- +: 100-200
- 0: 200-300
- -: 300-400
- - -: >400

Nonlinear stiffness In this case, stiffness refers to bending stiffness. A nonlinear angle stiffness curve can be beneficial in many applications, such as exoskeletons. A mechanism will score high if it is possible to tune the stiffness curve easily while scoring low if it is difficult.

Weight Weight can be crucial for certain applications, this is an important factor to consider. A seemingly heavy mechanism gets a lower score, a light mechanism a low score.

Dimensions Same as for weight, a crucial thing to consider in certain cases. A big, bulky system scores low, compact systems will score high.

Compatibility A measure of compatibility as a beam. Is there significant expansion in for example radial direction? Do the endpoints stay in roughly the same shape? A high score is given to mechanisms that behave like a regular beam or require minimal adaption to do so, while a low score is for mechanisms that require a complete overhaul of the mechanism or compatibility is impossible to achieve.

Development stage This criterion looks at the stage of the technology. A consumer-ready mechanism will score the highest while concepts and technologies without proof of concept will score the lowest. The score is based on the Technology Readiness Level (TRL) [2].

The grading system chosen is relative, mainly for two reasons. First, the mechanisms found all have completely different applications and scales, which makes comparing these with exact numbers of no importance. Secondly, most of the papers found do not focus on the bending and/or extending aspects. They are selected because it can be assumed that they have these properties. Each score will consist of a range between ++ and - - with 0 in the middle.

III. Results

In this section all the mechanisms found will be discussed. First, a short description and evaluation of each mechanism will be given. Then a comparison of the technologies will be done, followed by a conclusion and recommendation.

A. Metamaterials

Meta1: This article presents a deformable manipulator based on a human spine. The spine consists of several vertebrae with a backbone in the middle. The vertebrae are kept under tension with tendons. The tendons are attached on top and of the vertebrae and split into 3 sections: base, middle and distal. The whole mechanism can be actuated with a Teflon-PTFE transmission tube allocated inside the backbone. The vertebrae are not stiff in themselves, the stiffness comes from the tendons. There is however a possibility to adapt this to have a different coupling to allow the whole mechanism to bend due to the compliance of the vertebrae. The source does not mention any of this. Another great feature of the design is the nonlinearity of the stiffness. The stiffness can easily be adapted at different vertebrae by using a different stiffness tendon. It is also possible to implement nonlinear stiffness by adding a contact aided part between the vertebrae. A big disadvantage is the aforementioned possible disability to extend (due to the stiffness of the tendons determining the axial stiffness) and the weight and the volume of the total mechanism, which might be high. [4]

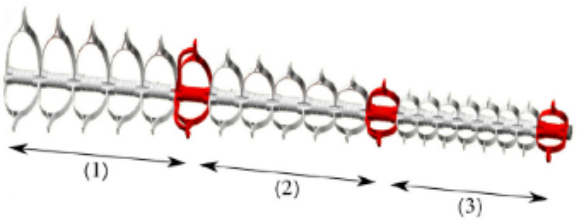

Fig. 1. Meta1 [4]

Meta2: This letter presents a Pneumatic Elastomer Robot (PER), called a Deterministically Adjusted Stiffness-Pneumatic Elastomer Robot (DASPER). It compromises a fused quadruple helix configuration encompassed by silicone. The purpose of this design is to transverse nontrivial trajectories and interact with the confined environment safely. It can do this by actuating it with pressure. Due to

the design of the helix, of which the stiffness can be altered locally, a certain path can be followed. One of the main advantages of this proposed design is that it can concurrently bend and extend and that the stiffness of the internal structures can be changed. As of now, the design is not suitable for an exoskeleton. It needs to be actuated to provide the modelled stiffness. Some kind of trigger mechanism might be able to do this. It is however very interesting to see that they can tune the axial and bending stiffness. This opens possibilities to use the design for all kinds of purposes. [28]

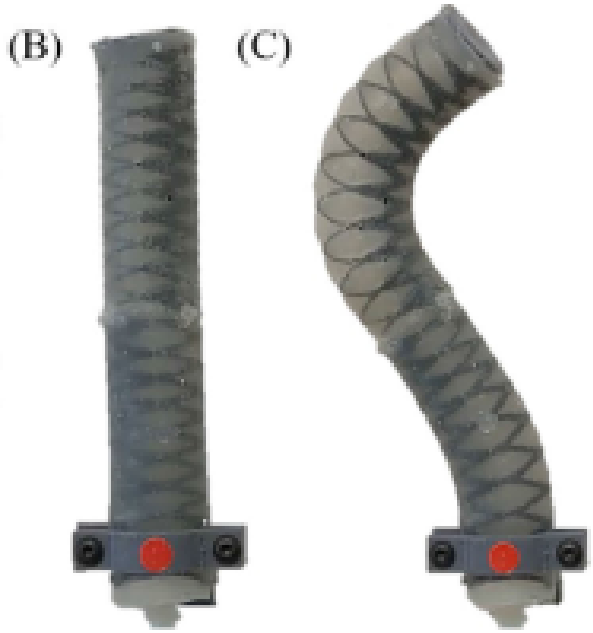

Fig. 2. Meta2 [28]

Meta3: In this paper, a new type of stiffener is proposed for a tube. This is in itself not an extendable system, but if one looks at just the stiffeners without the tube, it is apparent that this is what has been described in the method. A beam with a low cross-sectional area, but with a high (or relatively high) moment of inertia. From the proposed designs, d in the figure 3 looks the most promising. This could have the added advantage of working as flexures and thus being more flexible. It has an advantage for the implementation of the exoskeleton because it is just one beam that is easy to attach to the existing design without too much effort. [19]

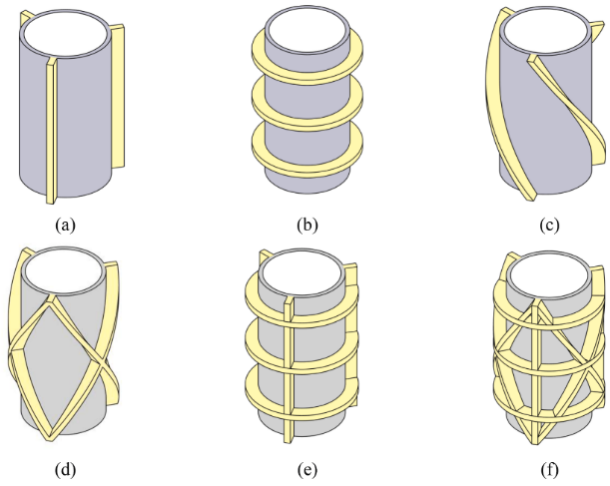

Fig. 3. Meta3 [19]

B. CAM

CA1: This paper describes a contact-aided compliant mechanism (CACM). It is flexible when bending in one direction and stiff when bending in the opposite direction. The spine consists of multiple 'blocks' with contact surfaces connected with compliant hinges. When bending the flexible way, all the stiffness comes from the compliant hinges. When bending the opposite direction stiffness comes from the compliant hinge and the beam that will form with the contact surface. This concept has one important feature. It splits the beam into multiple parts, while still keeping the same bending stiffness of the original beam. . By designing the flexures in such a way that extension is possible (by for example lowering the stiffness), the design complies with the goal of this literature review. This is of course speculation and there is no certainty this will work as intended. [23] [24]

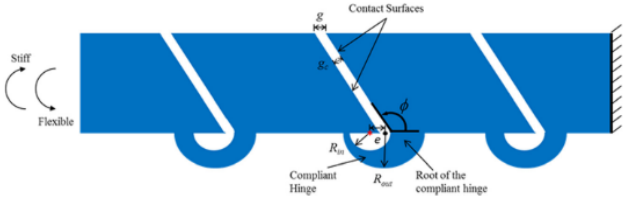

Fig. 4. CA1 [24]

CA2: This paper proposes a multi-contact aided continuum manipulator with anisotropic shapes. It consists of multiple disks with contact blocks

attached and 4 tendons running through the structure. The configuration of the contact blocks can be altered to change the stiffness and bending shape. Both the bending stiffness and the axial stiffness depend on the stiffness of the tendons in a positive correlation. This is undesirable but there are possibilities of adapting the proposed design. One could look at making the bending depend more on contact aided design. one way to do this is to make indents in the disk for the contact blocks to fit in. This way the axial stiffness will still be dependent on the stiffness of the tendons however the bending stiffness will depend on the stiffness of the tendons until contact is made and it will shift to the material stiffness. Of course, this is not a completed design and much is left to be desired, but there is certainly a possibility to explore. [1] Other similar mechanisms: [17]

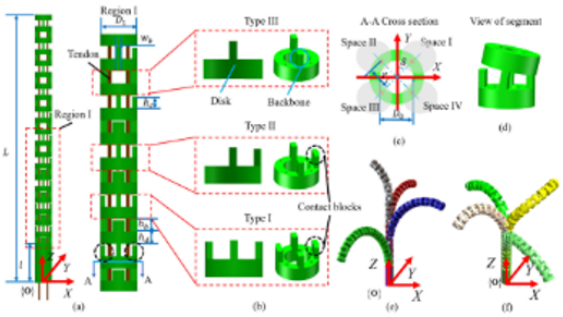

Fig. 5. CA2 [1]

CA3: This paper presents a mechanism to mimic finger motion with a contact aided compliant mechanism. The mechanism works by rolling one part over the other. Due to the shape of both a certain path is followed by the rolling part. This technique can be used to force the mechanism to extend. In the paper, they propose a four-bar linkage with a coupler. If there is a torsional spring attached to one of the joints in the four-bar linkage, the bending stiffness will increase independently of the axial motion. This technique gives multiple opportunities and new problems. The axial stiffness is not necessarily altered, but the path of the bending is. This is not entirely according to the goal of this review, but the technique could be valuable for an exoskeleton. A nice bonus is that it is easy to change the bending stiffness by just changing the torsional spring. The drawback is that the stiffness is not adaptable. [13]

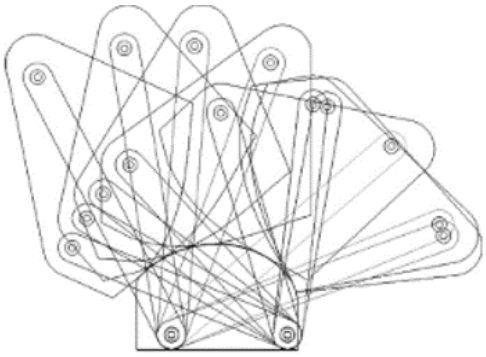

Fig. 4. Crossed fourbar linkage with coupler contacting ground.

Fig. 6. CA3 [13]

C. Origami

Ori1: Origami has been around for a very long time, but just in recent years mechanical properties and applications are being researched. One such research is the deployable stents. Stents are used to open up blocked lumen. As can be seen in this paper it is evident that when deploying the stent it will expand in the radial direction but also in the axial direction. They make use of different patterns on the inside and outside of the tube. The patterns are laser etched into the material. While this mechanism extends, the paper doesn't say anything about bending stiffness. Another thing is that it is self-deployable, which means that it will always push for the extended version.

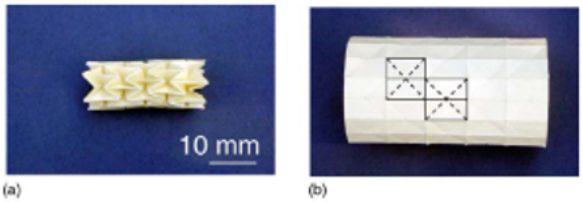

Fig. 7. Ori1 [9]

[9]

D. Granular Jamming

Gran1: This paper presents an exoskeleton for the hand utilizing granular jamming. Granular jamming is a physical phenomenon where pressure within a soft membrane is varied to cause a granular material to change from a fluid-like state to a

solid. In these types of systems, there is however need for a trigger that regulates the pressure. In this paper, they show a mechanism on top of a finger. Results are promising, but nothing definitive yet. The stretching is mentioned in the discussion, where they mention that it is not beneficial for the stiffness. This is because the longitudinal strain causes a significant number of the granules within the chamber to unlock from each other. This show that there is a possibility of extending, but with a lot of drawbacks. A better design of the granules could be the solution. [22]

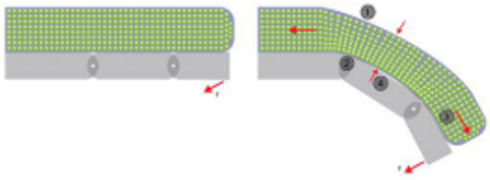

Fig. 8. Gran1 [22]

E. Other

Oth1: This paper proposes a new scissor mechanism design based on a rope structure. It consists of 2 scissor structures intertwined in an S-shaped linkage design. This way the deflection in horizontal configuration is reduced significantly. Another benefit is that several singularities are removed concerning the conventional scissor design. It claims 3 times less bending deformation than a parallel conventional scissor mechanism. A note to this is that the bending stiffness in a fully unfolded position is very low. The weight of the mechanism itself is already enough to push it down 10.65 mm. This is of course not desired when designing for an exoskeleton. The extension properties however are very good. It is a scissor mechanism, so that means it can extend multiple times its folded length. [21]

Oth2: This paper proposes a deployable Euler spiral connector that can span gaps between segments in a mechanism and then lay flat when under strain in a stowed position. This is not intended at all as an extendable mechanism, but it does work like one. In the unfolded position the middle sticks out a bit with respect to the outer two. In the folded position this difference is not there anymore. This is a neat incidental. What is a concern however

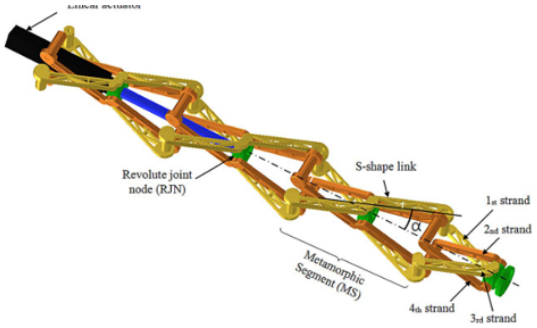

Fig. 9. Oth1 [21]

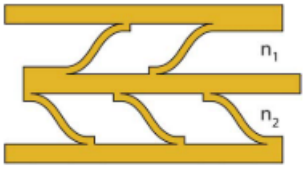

Fig. 10. Oth2 [27]

is the bending stiffness. The middle is connected with just too small flexures, of which the bending stiffness is questionable. This could be solved by adding a lot of them over the whole length of the beam or maybe adding something to connect the parts in another way without interfering with the motion. Once this is solved, the mechanism still expands and that is less ideal for an exoskeleton application. [27]

F. Comparison different technologies

All the technologies are compared using the table II with the performance criteria mentioned before.

Metamaterial shows great promise for nonlinear stiffness and adaptability. They can be fairly stiff and are compatible as a beam-like structure, which is useful in many applications. Metamaterials show great promise but there is certainly a research gap to explore. Contact aided mechanisms are a strange category as they have so many different designs and are most of the time mixed with the other classes. There are different designs reviewed and the beam-like designs show little promise in the axial stiffness category due to the use of tendons. CA3 is however interesting and could be a useful mechanism in some purposes where the path is already determined upfront.

TABLE II

COMPARISON OF TECHNOLOGIES

	Stiffness ratio	Nonlinear stiffness	Weight	Dimension	Compatibility	Development stage
Meta1	0	+ +	-	-	+	+
Meta2	0	+ +	+	0	+	+
Meta3	+	+	-	+	+ +	-
CA1	+	-	-	+	+	+
CA2	+	+ +	+	+	+	0
CA3	+ +	- -	+	+	0	+
Ori1	-	-	+ +	+	- -	-
Jam1	0	-	+	+	- -	-
Oth1	-	- -	-	-	0	+
Oth2	0	- -	0	-	- -	0

Granular jamming is an interesting concept, but has very few nonlinear stiffness possibilities and is in the early stages of development. It is also difficult to implement as a beam-like structure also because it is fairly weak in bending stiffness when not actuated. Actuation in itself poses another problem in itself, there has to be room to implement that in the design.

One thing noted during the search was that origami was less common to have a relatively high bending stiffness. This could be due to the creases not providing, or at most very minimal, bending stiffness. This is why most of them didn't cut the review. What origami excels in is the weight category. Origami is usually made of thin sheets folded in certain patterns, which makes it very lightweight. As of now, there is not enough research done to give a definite conclusion, but if the purpose of the mechanism is less dependent on bending stiffness origami certainly has its benefits.

IV. DISCUSSION

Using the axial-bending stiffness ratio a fair representation of the mechanisms is given. This way the potential of the mechanism is shown and the technique used can be implemented by others in their design. To improve the criteria, maybe some boundary conditions can be added. This paper looked at all the mechanisms, without discrimination. However, the way the stiffness ratio works a mechanism with almost zero axial stiffness would score fairly high while not having a lot of bending stiffness either. Boundary conditions could counter this but would exclude some mechanisms which could have the potential to be scaled to the required level. Adding an extra criterion of scalability could be added to address this.

In the classification, 4 main classes have been determined. They were the prevalent ones during the search and it is assumed that this is a fair representation. Whether this is true is up for question. The search is a difficult one, as there has been little research done in mechanisms with this specific characteristic. This means that to get to a suitable design, one needs to search for specific researches with the main goal not being related to the stiffness ratio. This is difficult as there are many solutions not known to the author. This is also a problem for the comparison. A lot of designs are not meant for the behaviour wanted in this review rather they are assumed to be able to. This makes the evaluation of the design very difficult as there is no value or exact data on the matter available. And this is just the problem for evaluation one design. Comparing them is even more difficult, as the application vary so much. As the application varies, the scale varies as well.

The classification serves its purpose in this paper but could be improved. The classes are clear and most of the time distinctive, but there are some overlapping parts especially with metamaterial and contact aided mechanisms. This makes it sometimes hard to see what is the cause of the low stiffness ratio. One could also argue that it is good to see how classes can be combined because they are not mutually exclusive.

Reflecting on the search, it can be said that there is almost no research into compliant slender

mechanisms with a low axial-bending ratio. The compliant part makes the problem a lot harder. There are for example extendable booms that could perform the task, but they are a lot heavier and have the tendency to revert to their shortest length if in an upright position. These drawbacks make the compliant part important. For future research it is recommended to further look in both the metamaterial and contact aided classes, as they are the most promising. What could also be interesting, and not found in the literature yet, is the coupling of the sides of the mechanism. During bending, one side of the mechanism compresses (the side in which the mechanism bends) and the other side will extend. For extending, both sides will extend. If one could make some kind of differential mechanism that will lock the movement when the sides have different states, so one compressing and one extending, and that allows the movement when they have the same state, so both extending or compressing, the problem will be solved.

One thing is certain, there are massive research gaps in this field. This is partly due to the problems mentioned above but also because of low interest or other solutions, like for example using a slider. It is however not always convenient to use such a mechanism so it is beneficial for the general knowledge to have more research into the subject of high bending, low axial stiffness.

V. Conclusion

The goal of this paper was to provide an overview of different slender mechanisms with low axial-bending stiffness ratio and compare them with each other. A classification has been made which can be used to identify promising techniques. To help with identifying the performance of the mechanism criteria are introduced. The most important criteria is the axial-bending stiffness ratio. This criteria ensures a fair comparison between the mechanisms. Each of the mechanism has been measured against the criteria and compared with each other. Metamaterials and contact aided scored the best overall, while combining techniques could prove fruitful for further research. Future research can be done in metamaterials to get a proper mechanism designed for the specific task of extending while keeping the bending stiffness. This could be combined with contact aided functions, as these show lots of promise as well. Origami also shows promise, but there is a lot of research still to be done in that field before a slender mechanism with low axial-bending stiffness ratio can be achieved.

References

[1] Xiaojie Ai et al. “A Multi-Contact-Aided Continuum Manipulator with Anisotropic Shapes”. In: *IEEE Robotics and Automation Letters* 6.3 (July 2021), pp. 4560–4567. DOI: 10.1109/LRA.2021.3068648.

[2] Katy Armstrong. “Emerging Industrial Applications”. In: *Carbon Dioxide Utilisation: Closing the Carbon Cycle: First Edition* (2015), pp. 237–251. DOI: 10.1016/B978-0-444-62746-9.00013-X.

[3] Robert P. Behringer and Bulbul Chakraborty. “The physics of jamming for granular materials: A review”. In: *Reports on Progress in Physics* 82.1 (2019). ISSN: 00344885. DOI: 10.1088/1361-6633/aadc3c.

[4] Thor Morales Bieze et al. “Design, implementation, and control of a deformable manipulator robot based on a compliant spine:” in: *https://doi.org/10.1177/0278364920910487* 39.14 (Apr. 2020), pp. 1604–1619. DOI: 10.1177/0278364920910487. URL: https://journals.sagepub.com/doi/full/10.1177/0278364920910487.

[5] Milan Dragoljevic, Salvatore Viscuso, and Alessandra Zanelli. “Data-driven design of deployable structures: Literature review and multi-criteria optimization approach”. In: *Curved and Layered Structures* 8.1 (Jan. 2021), pp. 241–258. ISSN: 23537396. DOI: 10.1515/CLS-2021-0022/MACHINEREADABLECITATION/RIS. URL: https://www.degruyter.com/document/doi/10.1515/cls-2021-0022/html.

[6] Ralph Hensel and Mathias Keil. “Subjective Evaluation of a Passive Industrial Exoskeleton for Lower-back Support: A Field Study in the Automotive Sector”. In:

https://doi.org/10.1080/24725838.2019.1573770 7.3-4 (Oct. 2019), pp. 213–221. DOI: 10.1080/24725838.2019.1573770. URL: https://www.tandfonline.com/doi/abs/10.1080/24725838.2019.1573770.

[7] Larry L. Howell, Spencer P. Magleby, and Brian M. Olsen. *Handbook of Compliant Mechanisms*. 2013. ISBN: 9781119953456. DOI: 10.1002/9781118516485.

[8] Karen Junius et al. "Bilateral, Misalignment-Compensating, Full-DOF Hip Exoskeleton: Design and Kinematic Validation". In: *Applied Bionics and Biomechanics* 2017 (2017). DOI: 10.1155/2017/5813154.

[9] Kaori Kuribayashi et al. "Self-deployable origami stent grafts as a biomedical application of Ni-rich TiNi shape memory alloy foil". In: *Materials Science and Engineering: A* 419.1-2 (Mar. 2006), pp. 131–137. ISSN: 0921-5093. DOI: 10.1016/J.MSEA.2005.12.016.

[10] Robert J. Lang. *The complete book of origami: step-by-step instructions in over 1000 diagrams: 37 original models*. Courier Corporation, 1988.

[11] Theodosia Lourdes Thomas et al. "Surgical Applications of Compliant Mechanisms: A Review". In: *Journal of Mechanisms and Robotics* 13.2 (Apr. 2021). ISSN: 19424310. DOI: 10.1115/1.4049491/1093979. URL: http://asmedigitalcollection.asme.org/mechanismsrobotics/article-pdf/13/2/020801/6660573/jmr_13_2_020801.pdf.

[12] Nilesh D. Mankame and G. K. Ananthasuresh. "Contact Aided Compliant Mechanisms: Concept and Preliminaries". In: *Proceedings of the ASME Design Engineering Technical Conference* 5 A (June 2008), pp. 109–121. DOI: 10.1115/DETC2002/MECH-34211.

[13] Yong Mo Moon. "Bio-mimetic design of finger mechanism with contact aided compliant mechanism". In: *Mechanism and Machine Theory* 42.5 (May 2007), pp. 600–611. ISSN: 0094-114X. DOI: 10.1016/J.MECHMACHTHEORY.2006.04.014.

[14] Matthias B. Näf et al. "Passive Back Support Exoskeleton Improves Range of Motion Using Flexible Beams". In: *Frontiers in Robotics and AI* 0.JUN (2018), p. 72. ISSN: 2296-9144. DOI: 10.3389/FROBT.2018.00072.

[15] Pierpaolo Palmieri et al. "A deployable and inflatable robotic arm concept for aerospace applications". In: *2021 IEEE International Workshop on Metrology for AeroSpace, MetroAeroSpace 2021 - Proceedings* (June 2021), pp. 453–458. DOI: 10.1109/METROAEROSPACE51421.2021.9511654.

[16] Edwin A Peraza-Hernandez et al. "Origami-inspired active structures: a synthesis and review". In: *Smart Materials and Structures* 23.9 (Aug. 2014), p. 094001. ISSN: 0964-1726. DOI: 10.1088/0964-1726/23/9/094001. URL: https://iopscience.iop.org/article/10.1088/0964-1726/23/9/094001%20https://iopscience.iop.org/article/10.1088/0964-1726/23/9/094001/meta.

[17] Zhongyuan Ping et al. "Design of Contact-Aided Compliant Flexure Hinge Mechanism Using Superelastic Nitinol". In: *Journal of Mechanical Design* 143.11 (Nov. 2021). ISSN: 1050-0472. DOI: 10.1115/1.4050750. URL: http://asmedigitalcollection.asme.org/mechanicaldesign/article-pdf/143/11/114501/6701970/md_143_11_114501.pdf.

[18] L. Puig, A. Barton, and N. Rando. "A review on large deployable structures for astrophysics missions". In: *Acta Astronautica* 67.1-2 (July 2010), pp. 12–26. ISSN: 0094-5765. DOI: 10.1016/J.ACTAASTRO.2010.02.021.

[19] Mojtaba Rafiee, Mehrdad Hejazi, and Hossein Amoushahi. "Buckling response of composite cylindrical shells with various stiffener layouts under uniaxial compressive loading". In: *Structures* 33 (Oct. 2021),

pp. 4514–4537. ISSN: 2352-0124. DOI: 10.1016/J.ISTRUC.2021.06.092.

[20] S. Mohammad Z. Sayyadan, Faezeh Gharib, and Alireza Garakan. "Granular jamming manipulator filled with new organic materials". In: *2017 22nd International Conference on Methods and Models in Automation and Robotics, MMAR 2017* (Sept. 2017), pp. 396–401. DOI: 10.1109/MMAR.2017.8046860.

[21] Bhivraj Suthar and Seul Jung. "Design and Bending Analysis of a Metamorphic Parallel Twisted-Scissor Mechanism". In: *Journal of Mechanisms and Robotics* 13.4 (Aug. 2021). ISSN: 1942-4302. DOI: 10.1115/1.4050813. URL: http://asmedigitalcollection.asme.org/mechanismsrobotics/article-pdf/13/4/040901/6724391/jmr_13_4_040901.pdf.

[22] Elliot Thompson-Bean, Oliver Steiner, and Andrew McDaid. "A soft robotic exoskeleton utilizing granular jamming". In: *IEEE/ASME International Conference on Advanced Intelligent Mechatronics, AIM* 2015-Augus (Aug. 2015), pp. 165–170. DOI: 10.1109/AIM.2015.7222526.

[23] Yashwanth Tummala et al. "Design and Optimization of a Contact-Aided Compliant Mechanism for Passive Bending". In: *Journal of Mechanisms and Robotics* 6.3 (Aug. 2014). ISSN: 1942-4302. DOI: 10.1115/1.4027702. URL: http://asmedigitalcollection.asme.org/mechanismsrobotics/article-pdf/6/3/031013/6252721/jmr_006_03_031013.pdf.

[24] Yashwanth Tummala et al. "Design optimization of a compliant spine for dynamic applications". In: *ASME 2011 Conference on Smart Materials, Adaptive Structures and Intelligent Systems, SMASIS 2011*. Vol. 2. 2011, pp. 743–752. ISBN: 9780791854723. DOI: 10.1115/smasis2011-5207.

[25] Nicholas Turner, Bill Goodwine, and Mihir Sen. "A review of origami applications in mechanical engineering:" in: *http://dx.doi.org/10.1177/0954406215597713* 230.14 (Aug. 2015), pp. 2345–2362. DOI: 10.1177/0954406215597713. URL: https://journals.sagepub.com/doi/full/10.1177/0954406215597713.

[26] Yang Xie and Kok Meng Lee. "Spine-Equivalent Beam Modeling Method with in Vivo Validation for the Analysis of Sagittal Standing Flexion". In: *IEEE/ASME Transactions on Mechatronics* 25.4 (Aug. 2020), pp. 2075–2087. ISSN: 1941014X. DOI: 10.1109/TMECH.2020.3007652.

[27] Collin Ynchausti et al. "Deployable Euler Spiral Connectors". In: *Journal of Mechanisms and Robotics* 14.2 (Apr. 2022). ISSN: 1942-4302. DOI: 10.1115/1.4052319. URL: http://asmedigitalcollection.asme.org/mechanismsrobotics/article-pdf/14/2/021003/6759446/jmr_14_2_021003.pdf.

[28] Uksang Yoo et al. "Analytical Design of a Pneumatic Elastomer Robot with Deterministically Adjusted Stiffness". In: *IEEE Robotics and Automation Letters* 6.4 (Oct. 2021), pp. 7781–7788. DOI: 10.1109/LRA.2021.3100608.

[29] Xianglong Yu et al. "Mechanical metamaterials associated with stiffness, rigidity and compressibility: A brief review". In: *Progress in Materials Science* 94 (May 2018), pp. 114–173. ISSN: 0079-6425. DOI: 10.1016/J.PMATSCI.2017.12.003.

[30] Igor Zubrycki and Grzegorz Granosik. "Novel Haptic Device Using Jamming Principle for Providing Kinaesthetic Feedback in Glove-Based Control Interface". In: *Journal of Intelligent & Robotic Systems 2016 85:3* 85.3 (June 2016), pp. 413–429. ISSN: 1573-0409. DOI: 10.1007/S10846-016-0392-6. URL: https://link.springer.com/article/10.1007/s10846-016-0392-6.

3

Research paper

Compliant slender mechanism with a low ratio of axial to bending stiffness

Stijn Houweling* Ali Amoozandeh* Just Herder*

***Abstract*— This paper proposes a concept for a compliant slender mechanism with a low axial-bending stiffness ratio. To obtain the desired behavior the axial stiffness is reduced by converting tension to bending stiffness of flexures. The bending stiffness is converted to the torsion and shear stiffness of the flexures. This results in a stiffness ratio of 8.5 for a model with a length of 0.25m. To evaluate the stiffness of the mechanism in an efficient way a Pseudo Rigid Body Model (PRBM) is developed. This model will be used with an optimization algorithm to minimize the stiffness ratio. A sensitivity analysis compares the PRBM and a Finite Element Method (FEM) model. Furthermore, a physical prototype is used to verify the results from the models.**

***Index terms* – Compliant mechanism, Axial Bending Stiffness Ratio, Extendable Mechanism**

I. Introduction

To design a lightweight mechanism several design principles can be used, one of which is a compliant mechanism. Compliant mechanisms are mechanisms that use elastic deformation to accomplish force and/or motion transmission [2]. Conventional mechanisms use hinges to connect rigid bodies to transfer either force and/or motion. Both have benefits and drawbacks and for compliant mechanisms, one of the useful properties is that the complexity is reduced and a smaller and lighter system can be produced [3].

Several compliant mechanisms use the spatial configuration to change the stiffness properties of the mechanism. For instance, zero stiffness compliant joints can be created by using pre-stressed compliant zero-free-length springs in a special arrangement [8]. Another example is the combination of a metamaterial and a compliant mechanism. Here the metamaterial is used to conform to the exact shape and stiffness of the elbow [13].

As seen, compliant mechanisms can be used to alter the stiffness properties. However, in the current literature, there has been little research into ratios between different stiffnesses. One such ratio is the axial-bending stiffness ratio. This is defined as the ratio between the axial stiffness, thus the longitudinal direction of a beam, divided by the bending stiffness. This ratio is independent of the material, and for a beam with a length of 1 m and a square cross-section with 0.01 m sides, the ratio is roughly 400. In general, the axial stiffness is higher than the bending stiffness for slender mechanisms.

One way to alter the ratio is by using flexures to convert the tension in a beam to the bending of flexures. This paper proposes such a mechanism, using flexures in different cells which are connected, in a similar fashion as a metamaterial.

The mechanism proposed in this paper could be used in several fields with each different applications. This could include space applications, where an antenna could be attached that can extend without the need for lubrication and is space efficient [11]. Another case could be as a linear guide [10]. A market that needs slender compliant low axial-bending ratio mechanisms is the passive back support exoskeleton market. Passive back exoskeletons can be used to reduce the load of labor for the user and prevent injuries in the long term [7] [6]. A problem occurring with such exoskeletons is due to the elongation of the spine during bending. When a user bends, the skin at the back tends to elongate, which has to be accounted for by the exoskeleton [4]. Current designs for exoskeletons use sliders [9] [5] [1] to account for this elongation, but these can be heavy, complex, and uncomfortable for the user. Here a slender mechanism with a low axial-bending stiffness ratio can be used. The relatively high bending stiffness lets the exoskeleton store energy in the system and reduces the load for the user while the low axial stiffness lets the user bend without compressing the spine.

The goal of this paper is to develop a slender compliant lightweight mechanism with a low axial-bending stiffness ratio. To obtain this goal and to make future designs easier, several steps are taken: (i) Make a suitable design, (ii) Develop a PRBM-based model to

Delft University of Technology, Department of Precision Mechanism Design

calculate the stiffness in both axial and bending directions, (iii) Make a suitable dimensional optimization algorithm. The PRBM-based model is useful for the design and optimization process, as it is less resource demanding than for example the FEM model.

Furthermore, a sensitivity analysis is done with the PRBM model and a FEM model to evaluate the variables and compare the models. After this, a physical prototype is made, which is then compared to both models. The mechanism is optimized for the use case of an exoskeleton using the dimensional optimization algorithm.

In chapter II the working principle is explained, along with the definition for the dimensions. In III the results from the PRBM model are compared to the prototype and a FEM model. Next to that, a sensitivity analysis is done for both the PRBM and FEM models. In IV the results are discussed and future research is suggested. Chapter V covers the conclusion of this paper.

II. Method

A. Working principle

The solution proposed in this paper consists of multiple cells connected linearly. The whole mechanism and a zoom-in of a cell are depicted in figure 1. A cell consists of vertical bodies connected by horizontal flexures. The mechanism can extend in the z-direction (axial) and bending will be done around the x-axis.

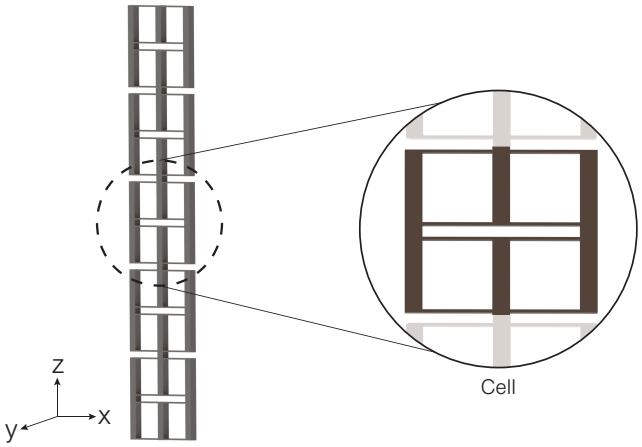

Fig. 1: Overview of the mechanism on the left, with a zoom-in of the mechanism on the right. Two flexures connect the rigid bodies.

By using the flexures in a horizontal configuration, the axial (Z) stiffness of the mechanism will decrease compared to a regular beam. This happens because the tensioning in the beam is converted to bending several small beams (the flexures). The wanted outcome is thus to convert the axial stiffness of the mechanism to the bending stiffness of the flexures.

A similar conversion happens for the bending (around the X axis) stiffness of the mechanism. The bending of the beam is converted to the torsion and shear stiffness of the flexures. To introduce the shear stiffness component 2 flexures have been used instead of 1. The distance between the flexures will influence the magnitude of the shear stiffness

In fig 2 the design variables are shown. For now, it is assumed that the vertical bodies are rigid. The design variables are the length (L_f), width (W_f) and thickness (t_f) of the flexures, the distance between the flexures (d_f) and the number of unit cells (# of stages). Each unit cell can have different values for the variables.

There are three other variables. The first is the distance between the sets. This is equal to the total length, L_total, divided by the number of stages. The second and third are the thickness (t_r) and the length (L_r) of the rigid bodies. The length of the rigid bodies is equal to $d_s + d_f + 2 * t_f$.

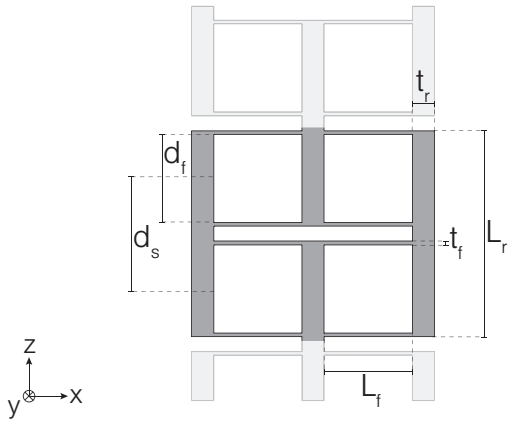

Fig. 2: The geometry of the model with all the variables. W_f is in the plane.

B. Modelling

To efficiently model a mechanism based on the design proposed in II-A, an analytic model is made based on the PRBM-model of Howell [3]. The model is made separately for the axial and bending stiffness.

Some definitions are needed for the model. The design is shown in figure 3. First, a distinction has to be made, namely that the horizontal parts are called

flexures, with subscript f, and the vertical parts are called rigid bodies, with subscript r.

There are also some definitions to be made on how to name the different collections of flexures. Two flexures together between the same rigid bodies are called a couple, subscript c. Together with the couple on the other side of the rigid body, they form a set, subscript s. Two sets connecting two different middle rigid bodies are called a stage, subscript st.

Then some subscripts related to the stiffness can be defined. If the variable is related to bending stiffness, the subscript is b. If the variable is related to axial stiffness the subscript is a and for torsion the subscript is t.

Furthermore, the assumption is made that a force is applied on the top of the mechanism. For the axial stiffness, there is a force applied in the direction of the positive z-axis. For the bending stiffness, the force is applied in the direction of the positive y-axis. The bottom of the mechanism is clamped.

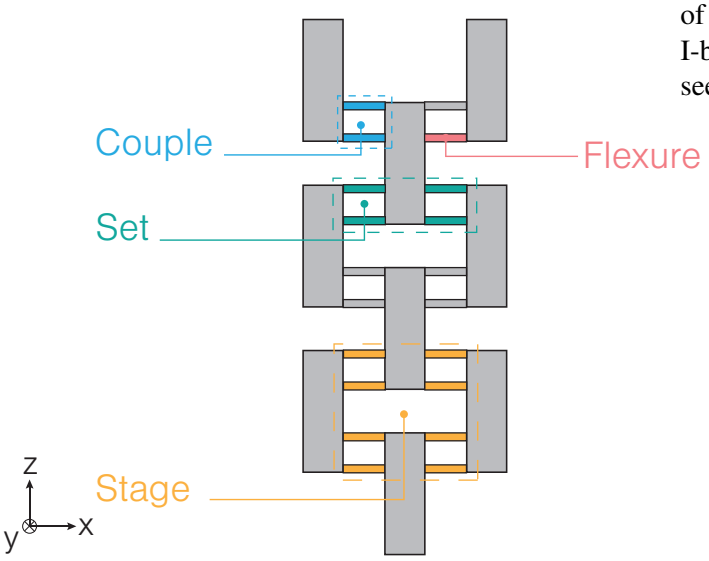

Fig. 3: Definitions of the model

Axial Stiffness: The axial stiffness of the whole mechanism depends on the bending stiffness of the flexures. The bending stiffness of one flexure is given by eq 1, where K_Φ is a constant equal to 2.65, γ is a constant for which the value is chosen to be 0.85, E is Young's modulus, I is the second moment of area and l is the length of the flexure.

$$K_f = 4 * \gamma * K_\Phi * \frac{E * I}{l} \quad [\mathrm{N/m}] \tag{1}$$

A couple is two flexures connected in parallel, the equivalent stiffness is the sum of both. This is also the case for the other couple of the same set. Thus the axial stiffness of 1 set is given by $2*2*K_f$. The different sets are connected in series, thus the equivalent stiffness of the whole mechanism can be given by.

$$K_{m,a} = \frac{16}{n} * \gamma * K_\Phi * \frac{E * I}{l} \quad [\mathrm{N/m}] \tag{2}$$

Where n is the number of sets.

Bending stiffness: To determine the bending stiffness, it is assumed that the whole mechanism is made up of rigid bodies connected by torsion springs. One torsion spring corresponds to one set of flexures. The deformations of these torsion springs can be added as they are in series. The deflections at the endpoint of all the couples are added together, after which the stiffness can be calculated by dividing the applied force by the total deflection. The stiffness of one couple of flexures consists of 2 components, torsion resistance, and shear resistance.

To calculate the torsion stiffness first the torsion constant is needed. To determine the torsion constant of a couple one calculates the torsion constant of an I-beam and subtracts the torsion constant of the web, see eq. 3a-3d.

$$J_{Ibeam} = (2 * W_f * t_f^3 + (d_f + t_f) * d_f^3)/3 \quad [\mathrm{m}^4] \tag{3a}$$

$$\beta = 1/3 - 0.21 * \frac{t_f}{d_f} * (1 - \frac{1}{12} * (\frac{t_f}{d_f})^4) \quad [\mathrm{m}^4] \tag{3b}$$

$$J_{mid} = \beta * t_f^3 * d_f \quad [\mathrm{m}^4] \tag{3c}$$

$$J_c = J_{Ibeam} - J_{mid} \quad [\mathrm{m}^4] \tag{3d}$$

This can then be used to calculate the rotation made by the set due to the torsion experienced using eq. 4, where T is the torsion on the set which is equivalent to the force applied times the distance to where the force is applied for a couple of flexures. This is important, as the torsion (or moment in the beam) will increase linearly with the length of the beam. After calculating the rotation of the couple, one can get the displacement on the endpoint of the mechanism.

$$\theta_{s,t} = \frac{L_f * T}{2 * G * J} \quad [\mathrm{rad}] \tag{4a}$$

$$Dy_{s,t} = \sin(\theta_{s,t}) * (L_{top}) \quad [\mathrm{m}] \tag{4b}$$

(4c)

The shear resistance is the other component of the bending stiffness. If one assumes the 2 flexures to act as springs in the x-direction, figure 4 is applicable. By use of superposition, the following equation for the displacement at the endpoint of the mechanism can be established, see eq. 5. Note that L_{arm} is the distance from the middle of the couple to the top of the mechanism.

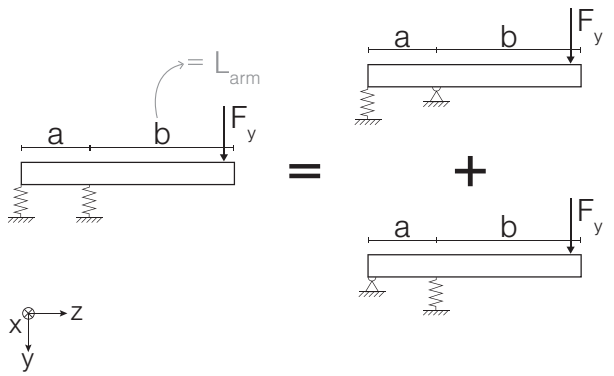

Fig. 4: Superposition principle of 2 flexures working to counter a force in the y direction.

$$a = d_f + t_f \quad [\text{m}] \quad (5a)$$

$$b = L_{arm} + 0.5 * t_f \quad [\text{m}] \quad (5b)$$

$$K_{c,s} = \frac{a^2 * K_{f,s}^2}{Kf,s * b^2 + K_{f,s} * (a+b)^2} \quad [\text{N/m}] \quad (5c)$$

$$x = \frac{F}{K_{c,s}} \quad [\text{m}] \quad (5d)$$

$$u = \frac{b * F}{a * K_{c,s}} \quad [\text{m}] \quad (5e)$$

$$\theta_{c,s} = \arcsin\left(\frac{u+x}{d_f + d_s + 2 * t_f}\right) \quad [\text{rad}] \quad (5f)$$

$$Dy_{c,s} = \sin(\theta_{c,s}) * L_{top} \quad [\text{m}] \quad (5g)$$

These calculations were all made with the assumption that the rigid bodies were rigid. During the comparison of the PRBM model with the FEM simulation, it has been found that there was a significant difference between the two. The main influence was the thickness of the rigid bodies (t_r). Thus, the rigid bodies are taken into account using Euler-Bernoulli beam equations.

The I of the beam depends on whether it is an inner or outer rigid body. It is assumed that the force and moment are applied at the top of the rigid body, in the middle of the couple. $Dy1_r$ is the translation of the rigid body. $Dy2_r$ consist of the deflection of the endpoint of the whole mechanism due to the rotation of the rigid body. See equation 6

If 2 outer beam:

$$I_r = 2 * 1/12 * t_r * W_f^3 \quad [\text{m}^4] \quad (6a)$$

If middle beam:

$$I_r = 1/12 * t_r * W_f^3 \quad [\text{m}^4] \quad (6b)$$

$$Dy1_r = \frac{Fy * L_r}{3 * E * I_r} + \frac{T * L_r^2}{2 * E * I_r} \quad [\text{m}] \quad (6c)$$

$$\theta_r = \frac{Fy * L_r^2}{2 * E * I_r} + \frac{T * L_r}{E * I_r} \quad [\text{rad}] \quad (6d)$$

$$Dy_r = Dy1_r + sin(\theta_r) * L_{arm} \quad [\text{m}] \quad (6e)$$

The total bending stiffness of the endpoint of the system due to a force applied at the top in the y-direction is given by eq 7. All the torsion springs are in series, thus the deflections can be added.

$$Ky_m = \frac{Fy}{\Sigma Dy_r + \Sigma Dy_{c,s} + \Sigma Dy_{s,t}} \quad (7)$$

C. Optimization

Dimensional optimization will be used to reduce the axial bending stiffness ratio, while still complying with the boundary conditions. The use case taken in this scenario is that of a compliant spine for an exoskeleton. This means that a certain amount of bending stiffness is needed to support the user and the axial stiffness should be as low as possible.

The design space is chosen in such a way that the exoskeleton can fit on the back of the user without hindering them. To make testing and prototyping easier, it has been chosen that the maximum length of the mechanism is 250 mm.

The optimizer will have separate design variables for each stage. One stage has 3 design variables (L_f , t_f, d_f). Due to production limitations, it has been chosen to limit the width of the mechanism to one value for all. This way the whole mechanism can be made out of one sheet of metal. A set of standard sheet thickness values has been determined and the optimizer will be put in a loop to determine the optimal value. The optimizer is put in a second loop to determine the optimal number of stages. After completion, it will run for n+1 number of stages, until a set limit is reached. The number of design variables for n number of stages and a certain width is $n * 3$.

The optimization will be done in MATLAB with fmincon, using the interior-point algorithm. It will be combined with the multistart function from MATLAB, with the option 'start points to run' set to bounds. This makes sure that all the start points are satisfying the boundary conditions.

The optimization problem is shown in eq 8. The main objective is to minimize axial stiffness. A force of 1N will be applied to the model in both the axial and bending direction. The first two constraints are related to bending deflection. For the use case, the bending deflection needs to have a certain value, target_Dy. To ease the task for the optimizer a tolerance is added, such that the first two constraints together give a range in which the Dy has to be satisfied. By using this constraint the bending stiffness is taken into account as this is directly linked to the deformation. The third and fourth constraints make sure that each of the couples has a rotational deformation that is within a range around the mean of all the rotational deformation from the couples. The PRBM model does not account for stresses, so using these two constraints makes sure that not all the deformation will occur in one couple. This is a way of accounting for the stresses. The model could still fail at the implemented load but is hypothesized to have better-distributed stresses. The optimized model will be checked in FEM software to see the stress distribution. Constraints one to four are all implemented as nonlinear constraints.

Boundary conditions will be applied to the optimizer as well. They can be seen in table I. The value of the width will be constrained to the value of the set currently calculated in the loop. The values of this set are based on the most common available sheets of material. The distance between the flexures is chosen as a function of the distance between the sets. The upper bound is set to a number smaller than 1 to account for the thickness of the flexures. This way the model generated will always be geometrically viable.

$$
\begin{aligned}
&\textbf{for} \quad nr\_stages = 4:10 \\
&\textbf{for} \quad W_f = \{0.002, 0.0025, 0.003, 0.004, 0.008\} \\
&\min_{t_f, L_f, d_f} \quad K_{m,a} \\
&\text{s.t.} \quad \frac{Dy - tol}{target\_Dy} - 1 \leq 0 \\
&\qquad \frac{target\_Dy}{Dy + tol} - 1 \leq 0 \\
&\qquad \frac{mean(D_\theta)}{(D_\theta(i) + tol)} - 1 \leq 0 \\
&\qquad \frac{D_\theta(i) - tol}{mean(D_\theta)} - 1 \leq 0 \\
&\qquad \text{boundary conditions for design var}
\end{aligned}
\tag{8}
$$

Design var	Lower bound	Upper Bound
W_f	$W_f(i)$	$W_f(i)$
t_f	0.0005	0.005
L_f	0.01	0.05
d_f	$\frac{L_t otal}{\text{nr\_ stages}*2} * 0.7$	$\frac{L_t otal}{\text{nr\_ stages}*2} * 0.92$
nr_stages	nr_stages(i)	nr_stages(i)

TABLE I: Boundary conditions values for the design variables

D. Model validation

To validate the PRBM model proposed, comparisons will be made with both a FEM model and a physical prototype, which will be explained in II-E. The FEM model will be made using the simulation study option in Solidworks, which uses solid elements. First, a sensitivity analysis will be done of the PRBM model and this will be compared to the results of the FEM model. The sensitivity analysis will be done for 5 variables: W_f, t_f, L_f, d_f,and nr_stages. The model will run for ranges shown in table II. One variable changes while the others remain on the base value. The graphs are generated for 50 points in the shown ranges. To limit the computation time the FEM model will run 8 times for each variable. For both the PRBM and FEM analysis the values of the design variables will be generated with the linspace function in matlab. The results will be shown in graphs in III.

Before it was mentioned that each stage has independent variables. Due to the number of variables needed to do so, it has been decided that all the stages have the same values for the design variables.

Another assumption is that the width is equal for the whole model, including the rigid bodies. This has been done such that there is no need to change the whole geometry of the FEM model and is more in line with the production method proposed later on.

Variable	Base Value	Range
W_f	0.004 m	0.001 - 0.01 m
t_f	0.001 m	0.0001 - 0.005 m
L_f	0.020 m	0.01 - 0.1 m
d_f	0.010 m	0.001 - 0.02 m
nr stages	5	1 - 10
t_r	0.005 m	-
L_{total}	0.250 m	-

TABLE II: Base dimensions used during the simulations, and the ranges for the sensitivity analysis. Each design variable except nr_stages will have the values for the range generated using linspace, with 50 points for PRBM and 8 for FEM.

E. Experimental validation

Prototype: The physical prototype will be made from grade 5 titanium. This material is chosen for its high elasticity and strength. Using the optimizer the values of the variables are generated, as given in III. The width of the prototype will be 0.004 m. The distance between the sets will be 0.025 m and the thickness of the rigid bodies will be 0.002m. The resulting prototype weighs 61 grams.

To make testing possible, the ends have attachment points. A waterjet cutter will cut a sheet of titanium in the desired shape. To prevent the water cutter from overshooting when rounding a corner, fillets have been added. These fillets have the extra benefit of providing extra stiffness and reducing stress build-up. The radius of the fillets is 0.0002 m. The final prototype can be seen in figure 5.

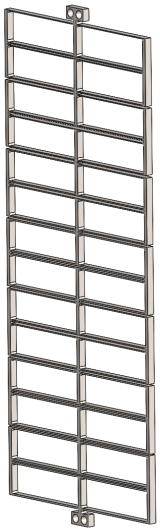

Fig. 5: The physical prototype used for the tests. The attachment points can be seen on the top and bottom.

Test setup: To test the model, a linear guide will be used to perform the motion. A force sensor is attached to the linear guide to measure the force. The output will be a force-displacement graph.

To measure the axial stiffness the bottom of the mechanism is clamped on one end and screwed on the force sensor on the other end, see figure 6. This will be done in a horizontal configuration due to limitations in the height. To screw the mechanism to the sensor a 3D printed attachment is used. The linear guide will move to the left and a force-displacement graph will be produced.

To measure the bending stiffness the mechanism will be clamped on one end and connected by a fishing wire to the force sensor on the other end, see figure 7. The configuration will be upside down, so the bottom of the mechanism will be on the top. This is again due to the limitations of the setup. The linear guide will move to the left and a force-displacement graph will be produced.

The desired angle is 25 degrees, so the mechanism will move 0.117 m to achieve such a deformation.

III. Results

A. Simulations

In figure 8 the relation between the design variables and the stiffnesses can be seen. For each graph, one of the variables is changed while the others remain constant. The base values can be found in table II. In the figures, the blue color represents the axial stiffness and the orange color represents the bending stiffness.

Var\Stage nr	1	2	3	4	5	6	7
t_f [mm]	0.9	0.8	0.6	0.8	0.6	0.5	0.5
L_f [mm]	50	50	50	50	50	50	50
d_f [mm]	15.5	15.5	15.5	15.5	15.5	15.4	16.1

TABLE III: Design variables of the prototype. Stage nr 1 is at the bottom and stage 7 is at the top.

Variable \Value nr	1	2	3	4	5	6	7	8	9	10
W_f	486.3	187.4	96.1	56.6	41.9	31.4	25.8	21.9	-	-
t_f	3.7	57.8	210.3	366.0	572.2	813.0	1087.2	1363.5	-	-
L_f	282.7	66.3	40.7	29.7	24.8	17.6	15.2	8.1	-	-
d_f	242.9	152.1	100.3	71.7	56.2	46.6	40.7	36.3	-	-
nr_stages	46.3	69.8	75.6	76.0	75.5	74.2	73.5	72.9	73.6	72.9

TABLE IV: The stiffness ratios for each of the design variables, corresponding with the FEM value of the graphs. The value nr corresponds to the values from linspace, with the first value nr the lowest value from the linspace.

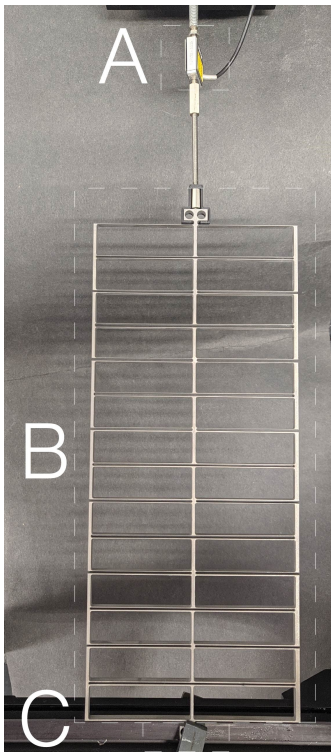

Fig. 6: Top-down view of setup to measure the axial stiffness. A: force sensor, B: prototype, C: clamp. Not shown is a linear guide that is attached to the force sensor.

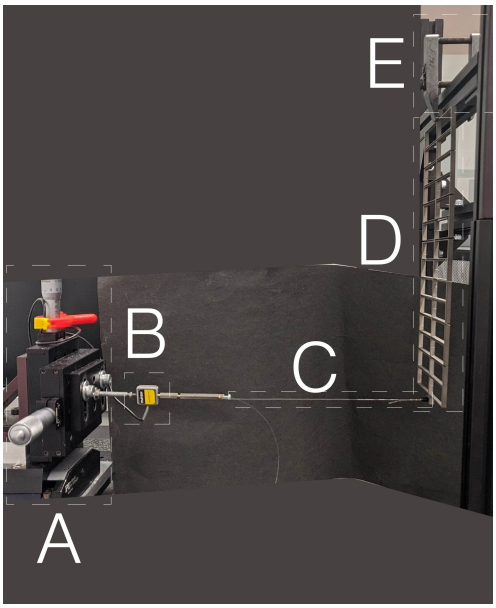

Fig. 7: Side-view of setup to measure the bending stiffness. A: linear guide, B: force sensor, C: nylon string, D: prototype, E: clamp

The solid lines are the results from the PRBM model and the * represents the results from the FEM model. The corresponding stiffness ratios which belong to the FEM model can be seen in table IV

In figure 8a the relation between W_f and the axial and bending stiffness can be seen. It can be seen that the axial stiffness has a positive linear correlation with the width of the flexures. Both models approximately give the same values. The bending stiffness has an exponential positive correlation with the width of the flexures. For W_f larger than 0.0005 m the curve of the PRBM model is steeper than the FEM model and the difference between the two increases. The graph shows that to get a higher stiffness ratio the width should be as large as possible because the bending stiffness is exponentially increasing.

In figure 8b the relation between t_f and the axial and bending stiffness can be seen. The FEM model has a positive linear correlation with the bending stiffness and a positive exponential linear correlation with the

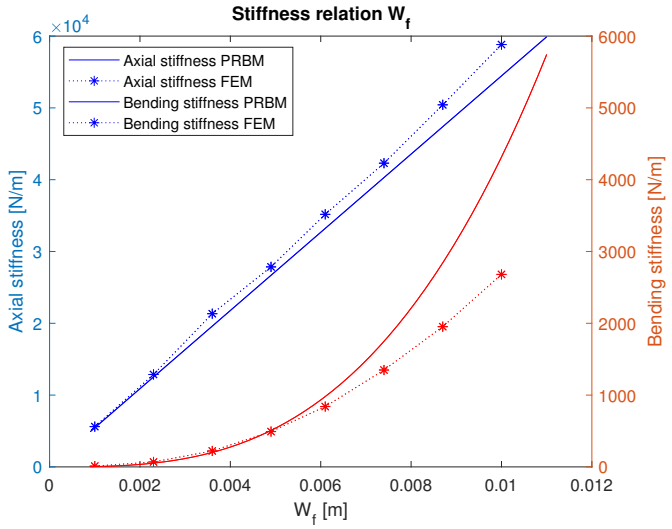

(a) Relation between stiffnesses and W_f

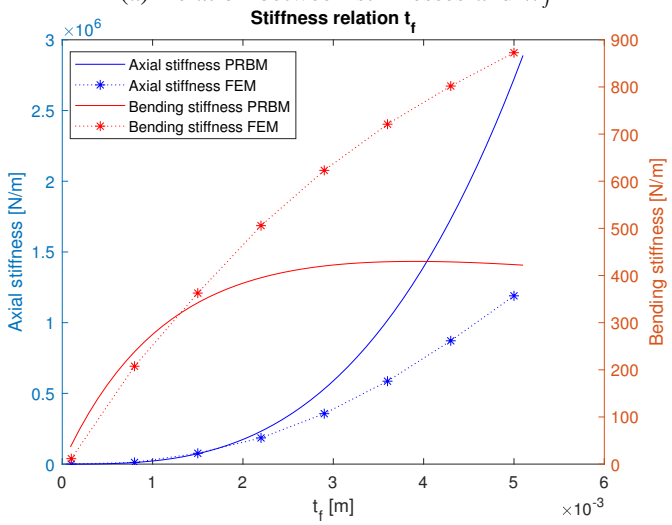

(b) Relation between stiffnesses and t_f

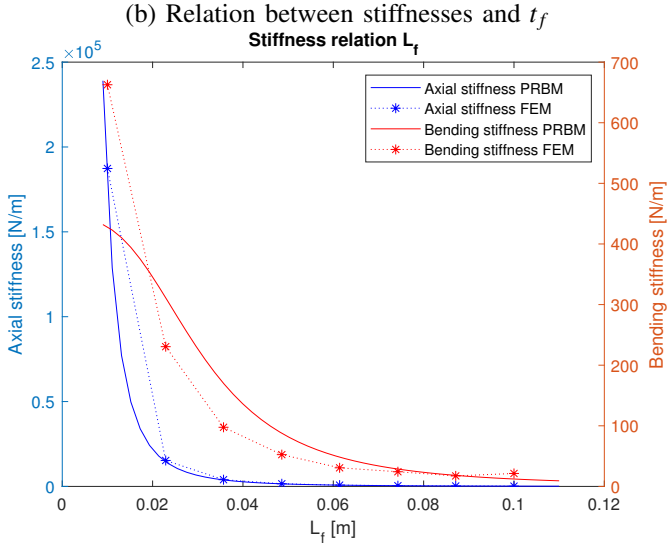

(c) Relation between stiffnesses and L_f

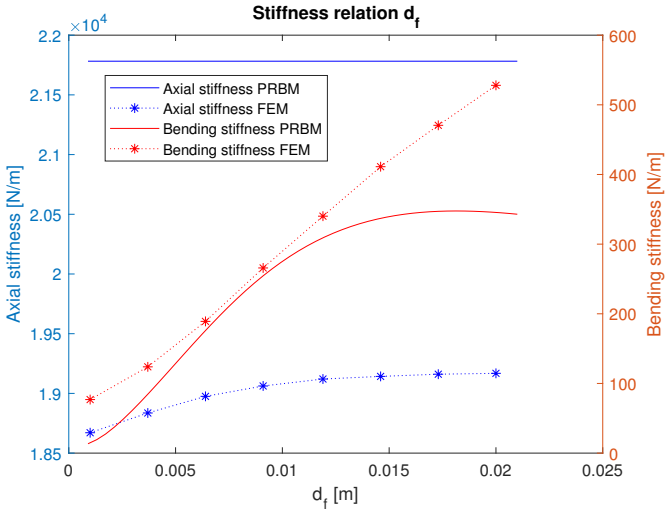

(d) Relation between stiffnesses and d_f

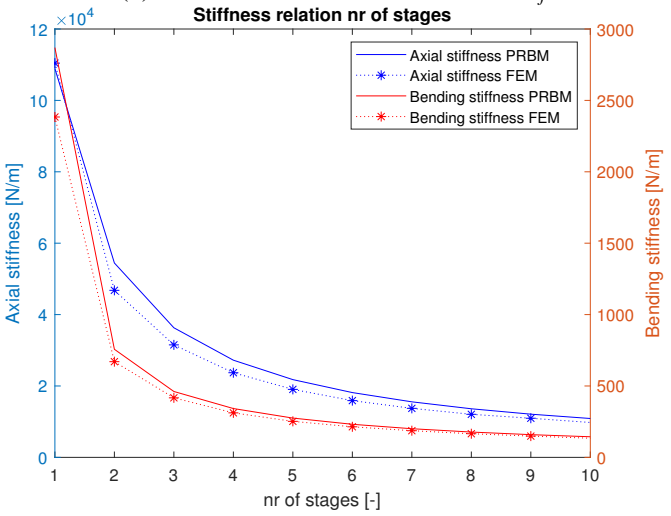

(e) Relation between stiffnesses and nr of stages

Fig. 8: Sensitivity analysis of both the PRBM and FEM model. The solid lines are the data gathered from the PRBM model and the asterisks are the data from the FEM model. Blue is the axial stiffness and red is the bending stiffness. On the left side of the figure is the axis for the axial stiffness, and on the right side is the axis for the bending stiffness. The design parameter is on the x-axis.

axial stiffness. The PRBM has a positive relation which levels out to a maximum for the bending stiffness and a positive exponential relation for the axial stiffness. It can be seen in the graphs that the FEM model differs from the PRBM model, especially for the bending stiffness. This difference is only when the thickness is larger than 0.0015 m. To lower the stiffness ratio the thickness of the flexures should be as small as possible.

In figure 8cthe relation between L_f and the axial and bending stiffness can be seen. For the axial stiff-

ness, there is a negative exponential correlation with the axial stiffness for both the PRBM and the FEM model. The axial stiffness is approximately the same for both models. For the bending stiffness, there is also a negative relation with the length for both the FEM and PRBM models. The FEM model has some outliers, but a decreasing trend. As can be seen in the table, the length of the flexures should be as large as possible such that the ratio is small. The reason is that the axial stiffness decreases faster than the bending stiffness.

In figure 8d the relation between d_f and the axial and bending stiffness can be seen. For the PRBM model, the axial stiffness is a constant value because the axial stiffness of the PRBM does not depend on the d_f. The axial stiffness for the FEM model lies approximately between 2.2E4 and 2.45E4 N/m. The bending stiffness is a positive linear relationship with the distance for the FEM model and a curve with a positive relation going to a maximum for the PRBM model. Up to 0.01 m, the difference between the FEM model and PRBM is not so much, but for larger values, the PRBM levels out. As can be seen in the table, the stiffness ratio increases with a larger distance between the flexures.

In figure 8e the relation between nr_stages and the axial and bending stiffness can be seen. Both the axial and bending stiffness show an exponentially decreasing trend. The results from the PRBM and the FEM model are comparable for both the bending and axial stiffness. It can be seen that the best ratio can be found within the lower number of stages. The difference is however small.

Overall the biggest differences in the ratio can be seen in the thickness of the flexures. The width is next in the improvements, while the length and distance between the flexures have roughly the same improvements for these ranges, while the nr_stages have little influence on the stiffness ratio.

B. Experiment

Figure 9a shows the results for the bending test, while figure 9b shows the results for the axial test. The bending stiffnesses of both the PRBM, FEM, and the physical experiment are shown in table V. In both figures it can be seen that the force-displacement graph is linear, meaning a linear stiffness profile. What also can be seen is that there is almost no hysteresis, as both graphs end at almost the same place.

During testing, it could be seen that most of the axial deformation occurred at the top of the mechanism, which was as expected. The flexures at the bottom of the mechanism are thicker and smaller than the ones on the bottom. This has been done to account for the stresses.

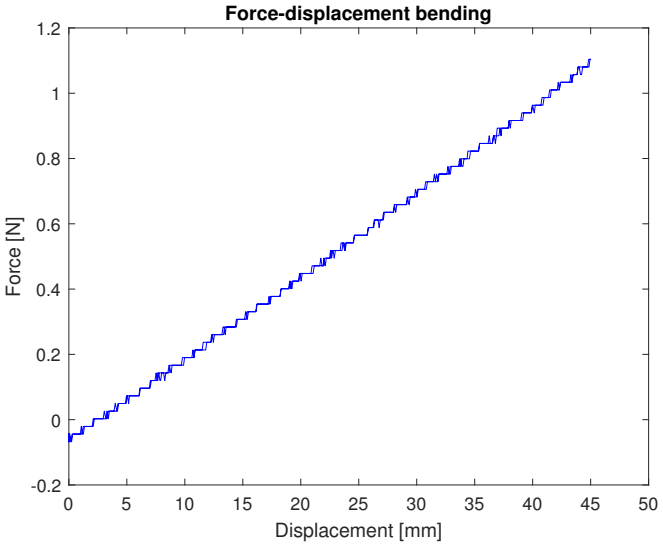

(a) Force-displacement graph for the bending stiffness

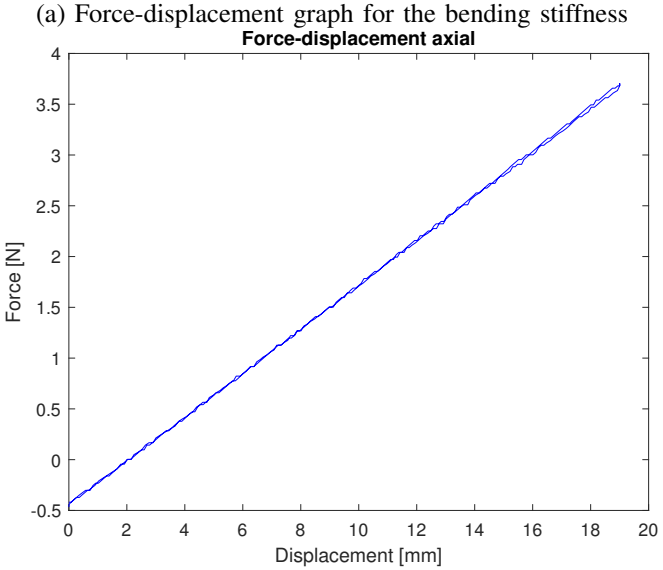

(b) Force-displacement graph of the axial stiffness

Fig. 9: Results from testing the physical prototype

The shape of the deflection during testing is shown in figure 10. The shape is fairly uniform which is as expected.

IV. Discussion

Functioning of the design

The expected behavior of the mechanism was found in both the simulated and experimental results. The mechanism can extend while also maintaining an axial-bending stiffness ratio below 10. This indicates that the working principle of using the bending stiffness of

	Kz [N/m]	Δ Proto [%]	Ky [N/m]	Δ Proto [%]	Ax/Bend ratio
PRBM	228.3	5.3	30.8	18.8	7.4
FEM	253.7	34.4	22.4	13.1	11.3
Proto	216.5	-	25.5	-	8.49

TABLE V: Results from each method for the physical prototype

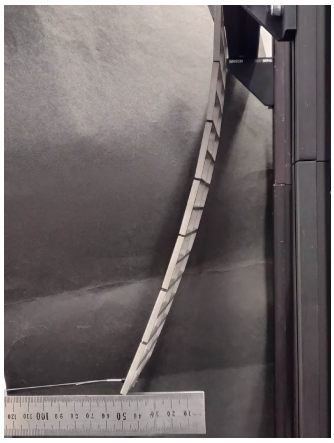

Fig. 10: Deformed shape when bending

the flexures as axial stiffness of the mechanism and using the torsion plus shear stiffness of the flexures as bending stiffness of the mechanism works.

In the design of the mechanism, 5 design variables have been addressed, but more variables influence the stiffness ratio. These are the total length of the mechanism and the thickness of the rigid bodies. When decreasing the total length the ratio will decrease and vice versa. The reason the total length was not considered as a design variable is that most designs have a pre-defined length for the mechanism. The thickness of the rigid bodies was not taken into account because the effect is considerably less than that of the others and it would make the optimization more difficult.

Comparison PRBM, FEM and Proto

As can be seen in the result section, the bending stiffness of the PRBM model and the prototype differ 18.8% from each other. The FEM model has a smaller difference with a maximum of 13.1%. This is fairly accurate for this scale. Several factors could cause this influence, as a result of inaccuracies in either the prototype, FEM model, or the PRBM model.

On the side of the prototype and testing, several factors could leave the results being inaccurate. One factor, for example, is the production of the prototype. The model was created using a waterjet which cut the prototype from one sheet of titanium. This is not a perfect manufacturing method, as the flexures are sometimes a bit thicker or thinner in some places. There are also some small imperfections made during cutting, which all could influence the results.

Another influence during the test setup is how the force is applied. When testing, the mechanism attachment point to the linear guide starts on the same level as the linear guide. When the linear guide moves the mechanism will bend, and this causes the mechanism to move upward. When this happens, the force will not be horizontal anymore. When the force is not horizontal part of it is used to extend the mechanism, which means that the stiffness will be lower as this is a less stiff direction.

Inaccuracies in the FEM model could also be a factor in the results. The size and shape of the mesh can influence the results, just as the model used. The model used is based on solids, which is appropriate in this case as the thickness/length ratio for the flexures is large (h/L $>$ 0.6) [**Akin**]. The size of the mesh was set to finest setting in Solidworks. The percentage of elements with an aspect ratio $<$ 3 was always larger than 95% and the percentage of elements with an aspect ratio $>$ 10 was always smaller than 0.1%. The maximum aspect ratio was between 10 and 20. All of these indicate a good mesh and give credibility to the FEM model.

What can be seen in 8 is that for t_f and d_f the bending stiffness goes to a maximum, while the FEM model is fairly linear. This indicates that there is some fault in the model. For the thickness, the model is valid for $t_f < 1.5mm$ but for larger values, it is not. One possible reason is the way the torsion stiffness is calculated. The flexures are modeled as an I-beam and the middle web is then removed. It is yet unknown what influence this has on the torsion stiffness at different values of thickness. Further research should be done to improve this part of the model.

The axial stiffness is mostly linear for the set range of d_f, but the bending stiffness levels out at roughly 0.012 m. Then the validity of the model stops. It is not known why this happens and further research should be done to assess this issue.

For the rest of the design variables, the model is valid

in the ranges shown.

For the axial stiffness, both models and the physical prototype show almost the same results. The FEM model has a higher stiffness, with a 17% difference, but the PRBM model is close with a 5% difference. The accuracy of the PRBM can partly be explained by how the PRBM model works. It is based on how beams bend in large deformations, and that is what happens when one extends the mechanism. There are a lot of flexures all just bending at the same time and this is exactly how the PRBM is supposed to be used.

One limitation of the PRBM model is that the only input is a force. Moments as input are as of yet not possible. Another limitation is

On a positive note, the PRBM can do a lot of calculations in a small time frame. To calculate the axial and bending stiffness of the prototype MATLAB takes 0.0013 seconds. Solidworks takes approximately 23 seconds to only calculate the bending stiffness. Designing for a purpose can be done quickly.

Future work

Recommendations for future work include improving the flexures. One way to do that is to use a different shape. In this design, the shape of the flexures was a straight beam. A different shape of the flexures, for example, a sinusoidal form could introduce different phenomena and thus alter the results [12]. Another idea is to change the angle of attachment of the flexures on the rigid bodies. Now the angle is 90 degrees, but it could be that a different angle might be better. One thing to note about this idea is that the axial stiffness probably increases. In the current design, the axial stiffness is dependent on the bending stiffness of the flexures. Changing the angle makes it more resistant to bending.

Another suggestion is to apply prestress to the flexures. This could decrease the bending stiffness but also decreases the torsion stiffness. More flexures could also improve the bending stiffness, but it is yet unknown how it will influence the axial-bending stiffness ratio.

V. Conclusion

In this paper, a slender compliant mechanism with a low axial-bending stiffness ratio is presented. The results show that (i) the design can achieve a low ratio, (ii) the PRBM-based model can accurately describe the said model, and (iii) the dimensional optimization works in reducing the stiffness ratio.

The mechanism showed the ability to extend while still being stiff in the bending direction. The main factor in this design is the design variable d_f, the distance between the flexures. This variable is independent of the axial stiffness but does influence the bending stiffness. Furthermore, a Pseudo-rigid body model (PRBM) was proposed to make the design of such a mechanism more convenient. A prototype was made from titanium and tested with an axial-bending stiffness ratio of 8.5, an axial stiffness of 253.7 N/m, and a bending stiffness of 25.5 N/m. The force-displacement graph obtained from these tests shows a linear stiffness profile when bending, with almost no hysteresis.

The prototype was compared with a FEM model and the PRBM. This shows that the PRBM has a very good approximation of the axial stiffness, with a difference of 5.3 %. FEM has a higher difference of 34.4%. For the bending stiffness, the PRBM is stiffer with an 18% difference from the 25.5 N/m stiffness of the prototype. The FEM model is also stiffer, with 13 % more stiffness. Overall the results are all within a 20% difference, which shows that the PRBM model is suitable to use for making a first design of the mechanism.

There have also been comparisons between the PRBM model and the FEM model. Here it shows that the PRBM has some limitations. For a large thickness of the flexures and a large distance between the flexures, the PRBM has a low bending stiffness.

References

[1] Mohammad Mehdi Alemi et al. “A passive exoskeleton reduces peak and mean EMG during symmetric and asymmetric lifting”. In: *Journal of Electromyography and Kinesiology* 47 (Aug. 2019), pp. 25–34. ISSN: 1050-6411. DOI: 10.1016/J.JELEKIN.2019.05.003.

[2] Larry L. Howell. “Compliant mechanisms”. In: (2001), p. 459. URL: https://www.wiley.com/en-us/Compliant+Mechanisms-p-9780471384786.

[3] Larry L. Howell, Spencer P. Magleby, and Brian M. (Brian Mark) Olsen. “Handbook of compliant mechanisms”. In: ().

[4] Kirsten Huysamen, Valerie Power, and Leonard O’Sullivan. “Elongation of the surface of the spine during lifting and lowering, and implications for design of an upper body industrial exoskeleton”. In: *Applied Ergonomics* 72 (Oct. 2018), pp. 10–16. ISSN: 0003-6870. DOI: 10.1016/J.APERGO.2018.04.011.

[5] Axel S. Koopman et al. “Biomechanical evaluation of a new passive back support exoskeleton”. In: *Journal of Biomechanics* 105 (May 2020), p. 109795. ISSN: 0021-9290. DOI: 10.1016/J.JBIOMECH.2020.109795.

[6] Michiel P. de Looze et al. “Exoskeletons for industrial application and their potential effects on physical work load”. In: *https://doi.org/10.1080/00140139.2015.1081988* 59.5 (May 2015), pp. 671–681. ISSN: 13665847. DOI: 10.1080/00140139.2015.1081988. URL: https://www.tandfonline.com/doi/abs/10.1080/00140139.2015.1081988.

[7] Paul Manns et al. “Motion Optimization and Parameter Identification for a Human and Lower Back Exoskeleton Model”. In: *IEEE Robotics and Automation Letters* 2.3 (July 2017), pp. 1564–1570. ISSN: 23773766. DOI: 10.1109/LRA.2017.2676355. arXiv: 1803.05666.

[8] Femke M. Morsch and Just L. Herder. “Design of a Generic Zero Stiffness Compliant Joint”. In: *Proceedings of the ASME Design Engineering Technical Conference* 2.PARTS A AND B (Mar. 2011), pp. 427–435. DOI: 10.1115/DETC2010-28351.

[9] Matthias B. Näf et al. “Passive Back Support Exoskeleton Improves Range of Motion Using Flexible Beams”. In: *Frontiers in Robotics and AI* 0.JUN (2018), p. 72. ISSN: 2296-9144. DOI: 10.3389/FROBT.2018.00072.

[10] Van Khien Nguyen et al. “Optimization design of a compliant linear guide for high-precision feed drive mechanisms”. In: *Mechanism and Machine Theory* 165 (Nov. 2021), p. 104442. ISSN: 0094-114X. DOI: 10.1016/J.MECHMACHTHEORY.2021.104442.

[11] L. Puig, A. Barton, and N. Rando. “A review on large deployable structures for astrophysics missions”. In: *Acta Astronautica* 67.1-2 (July 2010), pp. 12–26. ISSN: 0094-5765. DOI: 10.1016/J.ACTAASTRO.2010.02.021.

[12] Prabhu Shankar et al. “Design of Sinusoidal Auxetic Structures for High Shear Flexure”. In: *Proceedings of the ASME Design Engineering Technical Conference* 3.PARTS A AND B (Mar. 2011), pp. 63–72. DOI: 10.1115/DETC2010-28545.

[13] Lucas A. Shaw et al. “Computationally efficient design of directionally compliant metamaterials”. In: *Nature Communications 2019 10:1* 10.1 (Jan. 2019), pp. 1–13. ISSN: 2041-1723. DOI: 10.1038/s41467-018-08049-1. URL: https://www.nature.com/articles/s41467-018-08049-1.

4

Design case

This section gives additional information about the requirements and future recommendations for the exoskeleton design case. This specific case will handle the Laevo exoskeleton, with the differential mechanism designed by Robin Mak applied to it. A prototype will be made as a proof of concept, which will not be tested.

4.1. System requirements

An overview of the system requirements is shown in table 4.1. The most important requirement is that the axial stiffness is as low as possible while maintaining sufficient bending stiffness.

As mentioned before in the introduction, the human spine and skin elongate when bending. A back exoskeleton should also account for this extension. The total spinal surface elongation when lifting weight is between 30-70 mm, depending on the way of lifting and the weight [3]. This elongation is between the vertebrae C7 and S1. Because the mechanism only goes up to the shoulder blades and the lumbar region (lower back) accounts for 60% of the total elongation, the decision is made to set the goal of the total extension of the mechanism to 20 mm. To calculate the desired axial stiffness the desired force is also needed. The force chosen is 50 N, which makes the desired stiffness equal to 2500 N/m.

The first design of the mechanism for Laevo needs to provide 20Nm for a range of motion of 20 degrees. This translates to a force of 74 N at the top.

Further requirements include the design space. The spine should not hinder the user in its movements, thus a design space is required. The maximum width, which is for the most determined by the length of the flexures, is set to 0.14 m. This should be enough to not hinder the user when rotating or flexing the shoulders. Assuming that the rigid bodies will take up 0.015 m there is 0.065 left for the length of the flexures. The thickness of the spine, W_f in all the calculations, is determined by the plate of titanium bought. The plate is 4 mm thick, and there is room to cut 3 prototypes out of it which can be attached. This means that the thickness of the mechanism can have values of 4, 8, or 12 mm.

Exoskeletons have to be worn and carried by the user, thus need to be light to lower the strain on the user. Weight is thus an important requirement and should be as low as possible.

The manufacturing of the mechanism should be easy and cheap, and suitable for mass production. The material used should be non-corrosive and the produced model should not have sharp edges which can harm the user. The produced model should be durable enough to last 500.000 forward bends.

Type	Requirement	Specification
System	Axial stiffness	As low as possible, max of 50 N for 0.02 m extension which is 2500 N/m
	Bending stiffness	Support of 20 Nm for 0.27 m,
	Range of motion	Between 20-30 °when bending, between 0.0958 and 0.14 m deformation
	Stress	Distributed stress, may not lead to plastic deformation
	Weight	Lightweight system
User	Comfort	Not touching the user when bending, max width of mechanism 0.14m
	Safety	Safe material, no sharp edges
	Durability	Non-corrosive material, ability to last 500.000 forward bends
Manufacturing	Scalability	Ability to be scaled to large production
	Cost	Affordable

Table 4.1: Requirements for the design of the compliant spine

4.2. Realisation

To realize the compliant spine for the exoskeleton first the optimizer is run with the design constraints as mentioned before. The produced mechanism can be seen in 4.1 and the corresponding design variables in table 4.2. It has been made from 2 plates attached with bolts. This has been done because the plate thickness was only 4 mm while 8 mm was required according to the optimizer. On the top and bottom attachment points can be seen.

The distance between the sets is 15.625 which makes the total length including attachment points 269.4 mm. The thickness of the rigid bodies is 5 mm. The total weight of the mechanism, without the bolts and nuts, is 248.76 grams.

The design of Mak uses a joint at the bottom to attach the rod to the differential mechanism. This joint allows lateral (sideways) bending. As the spine mechanism designed has very limited flexibility in the lateral direction the joint will be used. The top of the rod is attached to a ball and socket joint. This allows for rotation in all directions and this is not a Degree of Freedom of the spine mechanism. To allow for rotations the ball and socket joint will stay.

Unfortunately due to some production issues and a limited amount of time, the prototype could not be made in time for the report. The reported axial stiffness of the mechanism according to FEM is 2737 N/m which just falls short of the desired stiffness, and the bending stiffness is 679.5 N/m. This means a bending deflection of 0.109 m when bending which is as required. The stiffness ratio is 4, which is a very good result. The mechanism does not exceed the yield stress during either bending or extending.

Variable \Stage nr	1	2	3	4	5	6	7	8
t_f [mm]	1.4	1.3	1.2	1.1	1.1	1	1	1
L_f [mm]	22.4	23.5	25.7	28.5	38	49	60	60
d_f [mm]	11.625	11.625	11.625	11.625	11.625	11.625	11.625	11.625

Table 4.2: The values of the design variables of the final design. Stage 1 is at the bottom and stage 8 is at the top

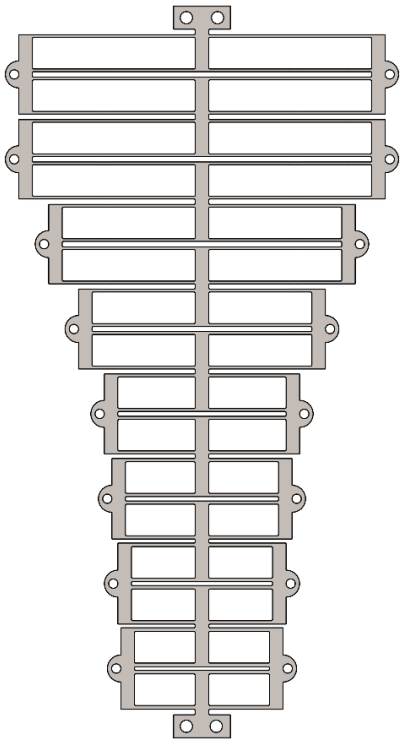

Figure 4.1: The final design of the prototype. The holes will be used to attach the 2 plates together with M3 bolts. The prototype will be attached to the rest of the exoskeleton using connection pieces from aluminum and the attachment points that can be seen at the top and bottom.

5 Discussion

The concept discussed and the application for the prototype show promise. The design process was difficult, as there were very few examples of a low axial-bending stiffness ratio that also were compliant. The solution proposed is a novelty in this application, although using flexures to have a low stiffness by using the bending stiffness is not a novelty, see for example linear motion systems. The most important discovery of the project is the independent variable, the distance between the flexures. This allows future research to easily influence the stiffness ratio.

Overall the project was successful, as a slender mechanism with a low axial-bending stiffness ratio suitable for use in an exoskeleton. The mechanism in the paper achieved a ratio of 8.5 while the ratio of the exoskeleton prototype was 4. The desired behavior was achieved and why that behavior happens is explained. Converting the bending of a beam to shear and torsion stiffness of the flexures while simultaneously converting the tension in the beam to the bending stiffness of the flexures is a main contribution of the project. The theory behind this can be used in future research and shows promise.

5.1. Design process

The combination of the dimensional optimizer with the PRBM model is useful in the design process, as the PRBM model has a significantly reduced computation time for the axial and bending stiffness when compared to the FEM model in SW. An important feature of the optimizer is an indirect measure for stress distribution, done by setting the angle of deformation for each of the sets of flexures to be almost equal. The constraint has been relaxed a bit to make it easier for the optimizer to find a suitable set of design variables. However, even with the relaxation finding is difficult for the optimizer and not always possible. The multitude of design variables combined with the nonlinear constraints is a cause for this. This has to be accounted for by the designer by relaxing some of the constraints.

A shortcoming of the PRBM model is that it does not take stresses into account. The optimizer uses the constraints to distribute parts of the stress, but it is never known if the model will yield under a certain force. The designer always has to use some other software to check if the stresses are within a reasonable range. As the optimizer and the PRBM model are not flawless it could be possible that the need arises for a slight improvement of the design variables. As mentioned in the paper, most of the axial deformation should occur at the top of the mechanism, while the bottom needs to be stiffer to withstand the larger moment there. The designer could see when using for example FEM software that there is room for improvement in the stress distribution and make the top flexures thinner for example.

5.2. Suitability for exoskeleton

The mechanism shows the desired behavior and is suitable to use in an exoskeleton. The axial stiffness of the mechanism is 2737 N/m, which is just short of required. There is some room for improvement as some flexures possibly could be made longer or thinner such that the mechanism does not fail, but this is a time extensive process in doing it by hand in the FEM software. Future work could improve some of it with an optimizer combined with a FEM model.

The bending stiffness of the exoskeleton prototype is 679.5, which is within requirements. The model does not fail, but the bending shape is not entirely uniform. The stiffness ratio of 4 is even better than the first prototype

and shows that the design is capable of achieving low axial stiffness ratios.

What is promising however is the weight of the exoskeleton. The total weight of the mechanism is 249 grams. This is a low value, as the current exoskeleton from Laevo weighs around 3 kg. This is an important selling point, as one of the reasons to make the design compliant and monolithic is to reduce the complexity and weight.

A great thing about the design is its simplicity and adaptability. It is possible to influence the bending shape by altering the values of the design variables of the different cells. This makes it suitable for exoskeleton use because the mechanism can be designed in such a way that it follows the shape of the human spine when bending.

The production of the prototype in the current design is relatively easy and cheap. The design is planar and 2D production methods are in general cheaper. Sheets of metal are widely available and waterjet cutting is a straightforward method of production that could be adapted to mass production. A note to this is that future designs would be better made if they were made from one sheet instead of 2 sheets attached. Using a thicker sheet could potentially reduce the quality of production of the waterjet cutter, as the water tends to deflect more for thicker sheets. If that is the case other methods of production should be considered. A disadvantage of the production method is the waste of material. Only a small part of the sheet gets used for the exoskeleton, the rest has to be thrown away or remelted into another sheet.

The material used is grade 5 titanium, which is the industry standard for titanium and thus widely available. A problem with grade 5 titanium is the price, as it is generally more expensive than spring steel which is used by Laevo. A big advantage however is that it is non-corrosive and non-toxic, which shows promise for exoskeletons that want to enter the medical market. Another advantage of using titanium is the high elastic strain.

The PRBM model could prove very useful for exoskeleton design. Humans have all different shapes and sizes which is making exoskeletons a difficult task. Using the PRBM model and the adaptability of the manufacturing, it should be possible to make a compliant spine mechanism tailored for the specific needs of the user. This could be a big advantage to an exoskeleton company, as this has not been possible in other designs.

5.3. Future work

The most important improvements for future work will concern the stiffness ratio. There are several paths to do so, as discussed in the paper. The flexures could take a different shape to improve the shear stiffness which will improve the bending stiffness. The incline of the flexures can also be changed which will improve the bending stiffness but lower the axial stiffness.

When looking at the design for the exoskeleton we see the twice the same design attached to make a thicker plate. A possible improvement could be to shift one of the plates a bit and attach it at different points. If done correctly it is hypothesized that the axial stiffness will not be influenced, as the number and shape of the flexures is not changed, but the bending stiffness could be improved by this shift because more support will be provided on weaker locations in the mechanism. When the mechanism bends, most of the bending deformation comes from the flexures while the rigid bodies stay relatively rigid. If the rigid bodies from two different stages are not attached but will touch each other while bending the model could be stiffer.

For future work, it will be important to look at the bending shape of the mechanism. This can be done by improving and adding to the existing dimensional optimizer. To make the exoskeleton fully compliant, the connection between the spine mechanism and the rest of the exoskeleton needs to be revised. The current connection between the spine mechanism and the differential mechanism consists of a hinge to provide a Degree of Freedom in the lateral bending direction. This could be replaced by for example a compliant prismatic crossed hinge. This hinge would experience a large moment so it has to be sturdy. The connection at the top of the spine, between the spine and the vest, is currently a ball and socket joint to allow torsion of the upper body and allow misalignment of the vest and spine. This could be replaced with a compliant spherical joint, but it is unknown if this would be overcomplicating the design.

6

Conclusion

This report shows the development of a slender compliant mechanism with a low axial-bending stiffness ratio suitable for use in an exoskeleton. A literature study was done to seek information about other designs and ideas with such a stiffness ratio. After that, a design is obtained showing the desired behavior, which can be seen in the paper. Using the expertise gatherer to design a general low axial-bending stiffness ratio mechanism, it was applied to the design case of an exoskeleton. The design case consists of the exoskeleton from Laevo with the differential mechanism from Robin Mak applied to it.

To get insight into the current status of research into axial-bending stiffness ratio, a literature survey has been done. Mechanisms that (possibly) exhibited this behavior were divided into categories. These categories are based on the type of mechanism. To determine the performance of the mechanisms each was evaluated on several criteria. The outcome of the literature review was that the most promising types of mechanisms are either metamaterials or contact-aided mechanisms. The survey also showed that little research has been done on the topic of low axial-bending stiffness ratio and that there is a research gap in this field.

The goal of the paper was to present a general slender compliant mechanism with a low axial-bending stiffness ratio. The paper first shows the PRBM-based model to describe the mechanism. This model has a reduced computation time for the axial and bending stiffness if compared to a FEM model. The optimization algorithm is presented and used to make a physical prototype from titanium. The result section is split into two parts. One is the sensitivity analysis, which compares the PRBM model with a FEM model and looks at the influence of each design variable on both the axial and bending stiffness. The second part of the result section compares the prototype and the FEM and PRBM models. The stiffness ratio achieved for the physical prototype is 8.5, which can be considered a very good result.

The design presented in the paper has been applied to the use case of an exoskeleton. The design variables were optimized such that the mechanism meets the requirements. A prototype has been made for the Laevo exoskeleton to take it one step further to a fully compliant exoskeleton. All the requirements have been met and the design shows promise for future development and improvements. A strong point of the design is the relatively easy production method and the ability to adapt it to the unique wishes of the customer.

A

Appendix A - Concept generation

To design an exoskeleton, one first has to consider the spine itself. It is important to see how a human bends and behaves to see how to design something for the spine. What immediately stands out is that the spine consists of multiple parts connected by soft tissue and muscles. Because of this, the spine can extend a bit, just as needed for the project. A prevalent idea during the concept generation was thus to make a design that consists of multiple elements that are connected in one way or another. Using this as inspiration multiple designs have been made, each of which will be explained in this section.

A.1. Concept A

The first concept is heavily inspired by the human spine. It consists of multiple rigid bodies that are connected by a soft tissue material. There is also the option to integrate extra cords. The idea is that there is movement possible in the z-direction due to the soft tissue having a low stiffness. But if one wants to bend the rigid bodies will touch each other and prevent the bending movement. This means that the mechanism has a low axial stiffness and high bending stiffness.

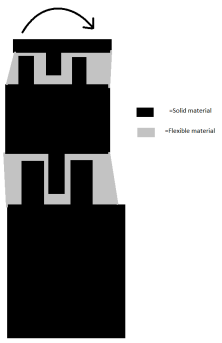

Figure A.1: Concept A, the grey part is a flexible material

A.2. Concept B

The second concept is based on a paper from Moon[8]. This paper proposes a finger mechanism based on a rolling element and a four-bar mechanism, see figure A.2. This mechanism has as property to extend when it bends. It forces the mechanism to bend. One could use this concept to attach a beam to this to force the extension or attach multiple of them to force the extension. This concept is very interesting but attaching multiple parts is almost impossible as they are based on a four-bar linkage system. Using only one of them on the bottom and a regular beam for the rest of the spine is a good idea, but there is no way to influence the bending shape of the mechanism. The extension is certainly there but forced and it can only be a fixed value. This might be difficult if one wants to squat or stoop, which both have different extensions for the spine.

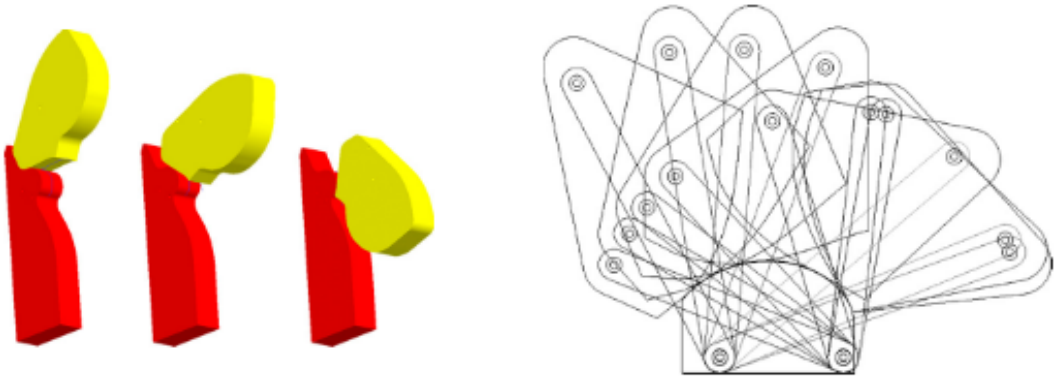

Figure A.2: The concept proposed by Moon [8]

A.3. Concept C

The third concept is based on a scissor mechanism, see figure A.3. This mechanism uses a special kind of scissor lift by using intertwined beams. It has a higher bending stiffness than a conventional scissor lift. This is a large design, which uses multiple moving parts. According to Suthar [9], it has a higher bending stiffness than a conventional lift but is still not adequate to be used as a spine in an exoskeleton. Another big drawback is all the moving parts, which also take up a lot of space on the back. That is not desired for an exoskeleton.

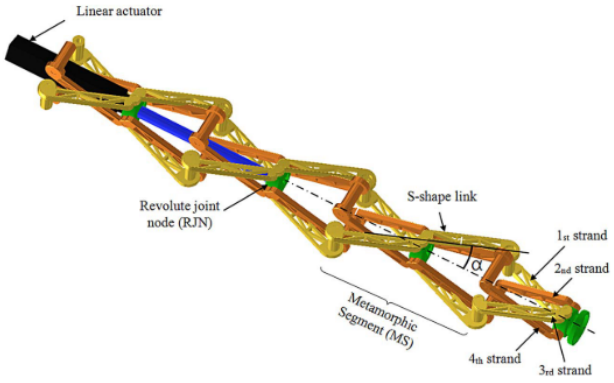

Figure A.3: Concept C as proposed by Suthar [9]

A.4. Concept D

This design uses horizontal flexures to convert tension in the beam to the bending stiffness of the flexures, see figure A.4. The first idea was to use one flexure, but then only the torsion stiffness of the flexures will be used as bending stiffness. By using a multitude, in this case two, flexures the shear force will also play a part in the bending stiffness. The mechanism should have a fairly okay bending stiffness, as the width does not change. The axial stiffness and bending stiffness are of course related, but it is hypothesized that distance between the flexures

does not influence the bending stiffness but will influence the axial stiffness.

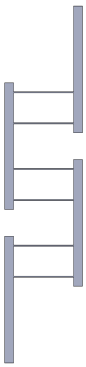

Figure A.4: Concept D, the width is in plane

A.5. Selection

A.6. Final design

After considering the concepts, it has been chosen to use concept D. This concept showed the most promise, and the others had problems and uncertainties. For concept A there were a lot of free moving parts which were connected with a soft tissue. This had a high chance of failure as the rotation point was not fixed and could be different each time when bending. Another issue is that bending and extending at the same time could prove difficult. Concept B is an option and certainly interesting, but a lot of stress would be applied to the flexures holding it together. Concept C has too many moving parts and the concern is that the mechanism will take up too much space. In the end, D seems the best choice, because it is a monolithic compliant mechanism and other mechanisms use the same principle of using the bending stiffness of flexures to allow movement.

To further investigate Concept D, multiple prototypes have been made with slight alterations. These alterations are for the 4 design variables that are hypothesized to have an influence on the stiffness ratio for 1 cell. These are the length, width, and distance between the flexures and the distance between the sets. For each design variable, one base value was set and one larger and smaller value was taken. The table with the values of the variables can be seen in table A.1. An important thing to note is that the distance between the sets was defined differently from the paper. The distance between the sets was the closest distance between the couples. The length of the rigid bodies was thus defined as $2 * d_f \; d_s$. At this stage, the thickness was considered a design variable, but not included because the 3d printers have limited accuracy. All these models were 3D printed to see the mechanism work. The print material was PLA.

Version	d_f [mm]	L_f [mm]	d_s [mm]	W_f [mm]
1	10	20	15	10
2	5	20	15	10
3	15	20	15	10
4	10	10	15	10
5	10	30	15	10
6	10	20	10	10
7	10	20	20	10
8	10	20	15	5
9	10	20	15	15

Table A.1: The iterations made of concept D. The first version is the base model.

After making the prototypes each was tested just by moving and pulling on it with the hands. The behavior could be seen and the important variables tested. The most important observations were:

- Most importantly, the mechanism seems to rotate around the z-axis when trying to bend. This is undesired behavior and should be fixed for the final model. An easy way to do this is by using flexures on both sides of the rigid bodies in the middle.

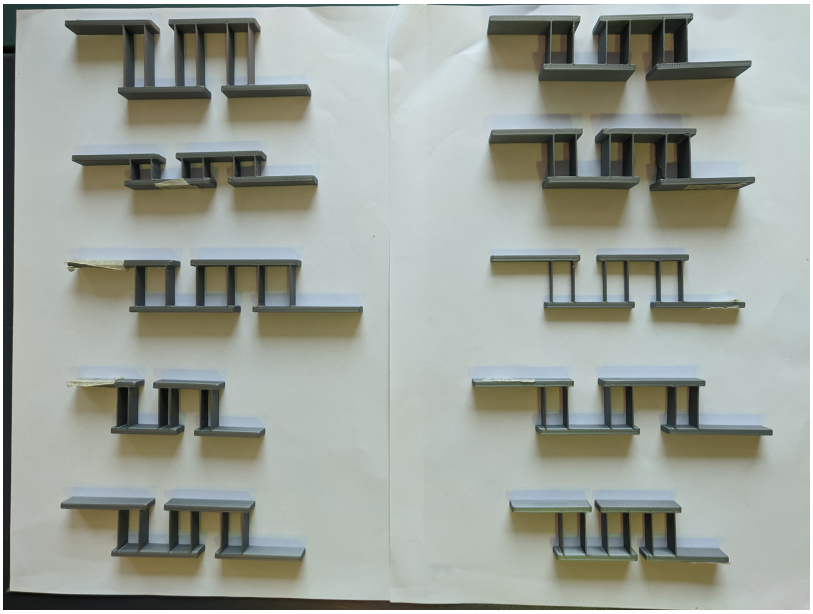

Figure A.5: Concept D with the different variables changed, number 1 is in the top left while 9 is in the bottom right

- When applying force on top of the mechanism in the y-direction, it can be seen that the rigid bodies barely deform, while the flexure experience torsion and shear deformation. Thus to improve the bending stiffness the shear and torsion stiffness of the flexures have to be improved. When only 1 flexure is used, the bending stiffness was low, thus most of the resistance comes from the shear part.
- The prototypes could break when applying somewhat higher forces, several broke during the testing. The breaking all occurred in the lower flexures because the moments in those flexures are the largest.
- The distance between the flexures has a lot of influence on the bending stiffness. For a large distance between the flexures, there will also be a larger bending stiffness. However, it has almost no influence on the axial stiffness. This is an important discovery, as it shows that there is a variable that is independent of the axial stiffness, thus it can be used to manipulate the ratio straightforwardly.
- The length of the flexures has a positive correlation with the axial stiffness and a negative correlation with the bending stiffness. The correlation with the bending stiffness is stronger.
- The distance between the sets does not influence the axial stiffness. It has to be noted that for small values the rigid bodies could touch each other, which should be addressed in the next iteration. The bending stiffness has a negative correlation with the distance between the sets, but for a good reason. Due to the definitions being made for the variables, decreasing the distance between the sets decreased the overall length. This resulted in a lower moment experienced by the flexures during bending, thus decreasing the stiffness. This is something that also should be addressed, as having multiple cells or stages attached will influence the overall length of the model greatly.

Considering all the points brought up above, the final design has been made, see figure A.6. An important improvement is including flexures on both sides of the middle rigid bodies. For the printing process, it was better to include small ridges at the outer end of the rigid bodies, these were removed for the titanium prototype which will be made after the optimization.

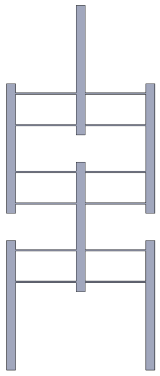

Figure A.6: The final concept with flexures on both sides

B

Additional Results

B.1. Stress results

In figure B.1 the von Mises stress plot can be seen from the prototype presented in the paper. This shows that the stresses in the flexures are well below the yield strength. The stress build-up is maximum around the connection between the flexures and the rigid bodies.

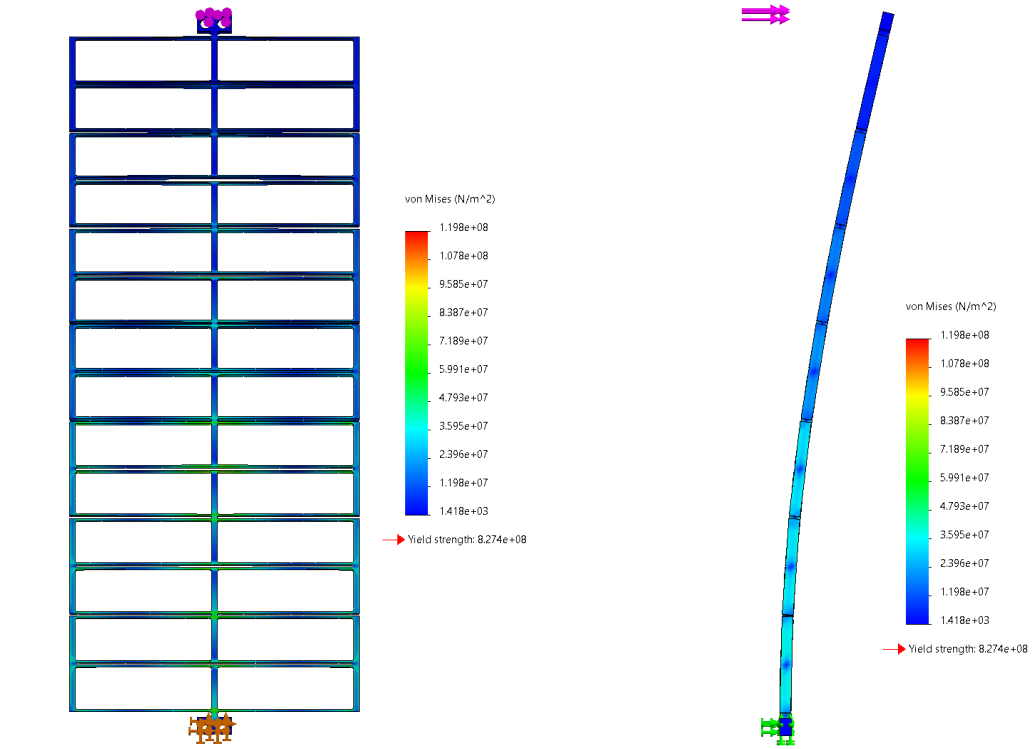

(a) Front view of stressplot

(b) Side view of stressplot

Figure B.1: Von Mises stress when applying 1 N on the first prototype

In figure B.2 the stress buildup and bending shape of the exoskeleton prototype can be seen. Keep in mind that these simulations were done without the bolts and assuming an 8mm thick model.

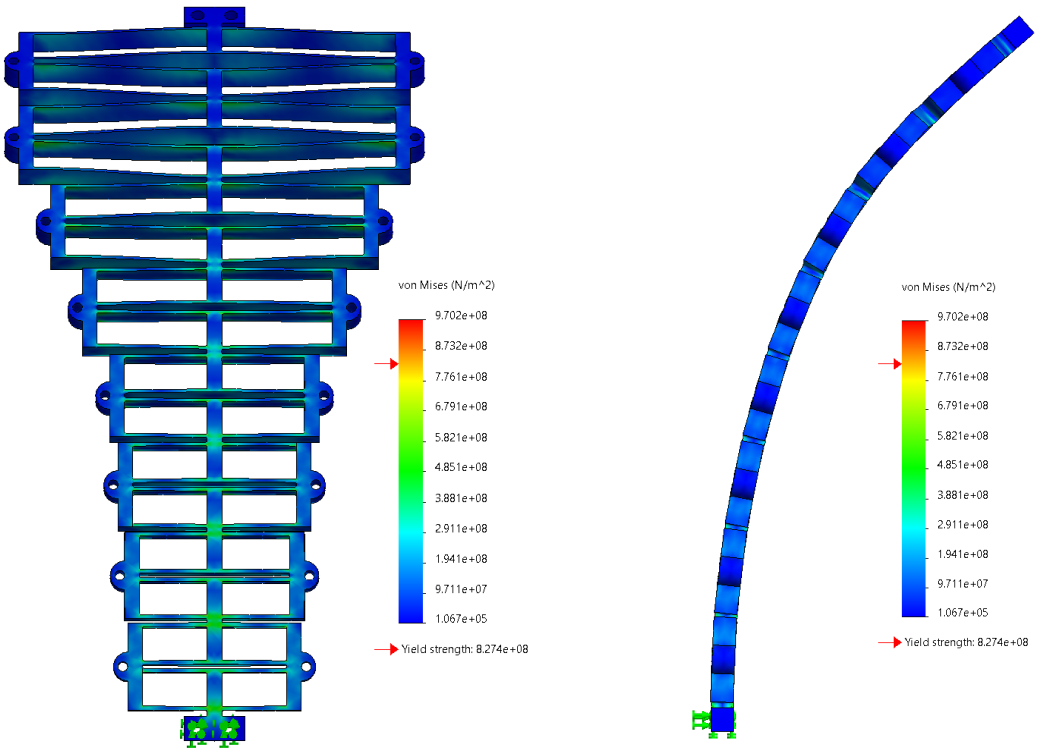

(a) Front view of stressplot

(b) Side view of stressplot

Figure B.2: Von Mises stress when applying 74N on the exoskeleton prototype

C

Appendix F - Code

C.1. Calculate axial stiffness

```
1       function K_ax = K_ax_setfun_prot2_V2(W_flex,t_flex,L_flex,parms)
2       K_ax_bottom = 0;
3       for i = 1:length(t_flex)
4       I_bendax    = 1/12*W_flex(1)*t_flex(i)^3;
5       K_ax_flex   = 4*parms.gamma*parms.K_phi*parms.E*I_bendax/(parms.gamma^2*L_flex(i)^3);
6       K_ax_bottom = K_ax_bottom+2*1/(2*parms.nr_flex*K_ax_flex);
7       end
8
9       K_ax    = 1/K_ax_bottom;
10      end
```

C.2. Calculate bending stiffness

```
1       function [K_bend,Dtheta,Dy] = ...
            K_bend_setfun_prot2_V4(W_flex,t_flex,L_flex,dist_flex,parms)
2   Dy = 0;
3   Dtheta = [];
4   T = [];
5   Dy_rigid_ = 0;
6   K_bend_bottom = 0;
7   for i = 1:length(L_flex)
8
9   %% Bending stiffness, Attempt to solve problem with the I-beam approach
10
11  %stiffness for the shear bending
12  I_bendbend  = 1/12*t_flex(i)*W_flex(i)^3;
13  K_bend_flex = ...
        4*parms.gamma*parms.K_phi*parms.E*I_bendbend/(parms.gamma^2*L_flex(i)^3); % [N/m] ...
        stiffness in the shear direction of one flexure
14
15  L_arm = parms.dist_set;
16
17  position = ...
        [0,1;2,3;4,5;6,7;8,9;10,11;12,13;14,15;16,17;18,19;20,21;22,23;24,25;26,27;28, ...
        29;30,31;32,33;34,35;36,37;38,39];
18
19
20      for j = 1:2
21          T(i,j) = parms.Fy*(position(i,j)*L_arm+0.5*dist_flex(1)+t_flex(1));
22          %torsion part
23          a = dist_flex(i)+t_flex(i);
24          % b = parms.dist_set-0.5*dist_flex(i)-0.5*t_flex(i);
25          b = position(i,j)*L_arm+0.5*t_flex(1);
```

```
26
27          K_bend1     = (a^2*K_bend_flex^2)/(K_bend_flex*(b)^2 ...
28                + K_bend_flex*(a+b)^2);
29
30
31
32
33
34
35          %shear part
36          if position(i,j) == 0    % Deflection at top stage
37
38              Dtheta_bend = 0;
39
40
41          else
42
43
44              x_bend = parms.Fy/(2*K_bend1);                                          ...
                    % [m] deflection of endpoint of 1 stage
45              u1_bend = parms.Fy/K_bend_flex*(b/a);                                % ...
                    [m] deflection of bottompoint of rigid body (furthest away from source)
46              Dtheta_bend = asin((u1_bend+x_bend)/(b));                  % [rad] ...
                    deflection angle due to shear force
47          end
48
49          J_Ibeam     = ...
                (2*W_flex(i)*t_flex(i)^3+(dist_flex(i)+t_flex(i))*dist_flex(i)^3)/3;
50          b           = t_flex(i);
51          d           = dist_flex(i);
52          beta        = 1/3-0.21*(b/d)*(1-1/12*(b/d)^4);
53          J_mid       = beta*b^3*d;
54          J           = J_Ibeam-J_mid;
55
56
57
58
59          Dtheta_tors = L_flex(i)*T(i,j)/(2*parms.G*J);
60          Dy_tors = sin(Dtheta_tors)*(position(i,j)*L_arm+0.5*dist_flex(1)+t_flex(1));
61          K_tors = parms.Fy/Dy_tors;
62
63
64          K_bend_bottom = K_bend_bottom + 1/(2/(1/K_bend1+1/(2*K_tors)));%+2*K_tors);
65          %"rigid body" deformation adding to that
66          if  rem(position(i,j), 2) == 0
67              I_rigid = 2*1/12*parms.t_rigid*W_flex(i)^3;
68          else
69              I_rigid = 1/12*parms.t_rigid*W_flex(i)^3;
70          end
71          Dy_rigid_F = parms.Fy*parms.L_rigid(i)^3/(3*parms.E*I_rigid);
72          Dy_rigid_M = T(i,j)*parms.L_rigid(i)^2/(2*parms.E*I_rigid);
73
74          Dy_rigid = Dy_rigid_F + Dy_rigid_M;
75
76          if position(i,j) == parms.nr_sets*2-1
77              Dy_rigid = 0;
78          end
79
80          Dtheta_rigid = parms.Fy*parms.L_rigid(i)^2/(2*parms.E*I_rigid) + ...
                T(i,j)*parms.L_rigid(i)/(parms.E*I_rigid);
81          if position(i,j) == parms.nr_sets*2-1
82              Dtheta_rigid = 0;
83          end
84
85          Dy_rigid_ = Dy_rigid_ + sin(Dtheta_rigid)*(position(i,j)*(L_arm))+Dy_rigid;
86          %add both of them together
87          Dy = Dy + sin(Dtheta_bend)*(position(i,j)*(L_arm)+0.5*dist_flex(1)+t_flex(1)) ...
88               + sin(Dtheta_rigid)*(position(i,j)*(L_arm))+Dy_rigid;              % [m] ...
                    total deflection at endpoint due to set of flexures
89      end
90
```

```
91 end
92
93 % K_bend = 1/K_bend_bottom;
94 K_bend = parms.Fy/Dy;
```

C.3. Parameter file

File needed to run both the axial and bending stiffness functions

```
1      W_flex      = x(1,:);
2      t_flex      = x(2,:);
3      L_flex      = x(3,:);
4      dist_flex   = x(4,:);
5      parms.nr_sets = x(5);
6      L_total     = 0.27;
7      parms.dist_set    = L_total/(parms.nr_sets*2);
8      parms.L_rigid = dist_flex+parms.dist_set+2*t_flex;
9      parms.t_rigid = 0.01;
10
11
12     parms.nr_flex = 2; %per set, only the axial stiffness is dependent on this.
13
14     parms.gamma = 0.85;
15     parms.K_phi = 2.65;
16
17     % Spring steel
18     % parms.E = 190e9;
19     % parms.G = 72e9;
20
21     %titanium Ti-6Al-4V
22     parms.E = 104.8e9;
23     parms.G = 41e9;
24
25     parms.Fy = 60;                                          %[N] Force applied, y ...
           direction
26     parms.Fz = 10;
27
28     parms.desired_dz = 0.010;
29     parms.desired_angle_low = 20*pi/180;
30     parms.desired_angle_up = 30*pi/180;
31     parms.tol_flex = 0.0004;
32
33     parms.desired_Dy_up = sin(parms.desired_angle_up)*(L_total+parms.desired_dz);
34     parms.desired_Dy_low = sin(parms.desired_angle_low)*(L_total+parms.desired_dz);
35
36
37     parms.desired_Dy_tol = 0.01;
38     % parms.desired_K_bend = 400;
39
40     %values to make the angle equal
41     parms.angle_tol = 0.01; %tolerance for the equality of the angles
42     parms.angle = 0.09;
```

C.4. Optimization files

Main code for the optimizer:

```
1      %% working with variable nr_sets
2      %works perfectly
3      %full scale model
4
5      % prot2_params2
6      t_plate = [0.004 0.008 0.012];
7      for j = 2:3
8      for i = 4:10
9      parms.nr_sets = i;
```

```

    W_flex_ = t_plate(j)*ones(1,parms.nr_sets);
    t_flex_ = 0.0013*ones(1,parms.nr_sets);
    L_flex_ = 0.01*ones(1,parms.nr_sets);
    dist_flex_ = (0.27/(2*parms.nr_sets)-0.015)*ones(1,parms.nr_sets);

    x0 = [W_flex_;
        t_flex_;
        L_flex_;
        dist_flex_
        parms.nr_sets*ones(1,parms.nr_sets)]; %x0 for all design var [W_flex; t_flex; ...
            L_flex; dist_flex]


    options = ...
        optimoptions('fmincon','Algorithm','interior-point','MaxFunctionEvaluations', ...
        40000 ,'MaxIterations',2000);

    fun = @(x)prot2_obj2(x);
    A = [];
    b = [];
    Aeq = [];
    beq = [];


    lb = [t_plate(j)*ones(1,parms.nr_sets);
         0.001*ones(1,parms.nr_sets);
         0.01*ones(1,parms.nr_sets);
         (0.27/(2*parms.nr_sets)-0.01)*ones(1,parms.nr_sets);
         parms.nr_sets*ones(1,parms.nr_sets)];

    ub = [t_plate(j)*ones(1,parms.nr_sets);
        0.005*ones(1,parms.nr_sets);
        0.06*ones(1,parms.nr_sets);
        (0.27/(2*parms.nr_sets)-0.01)*ones(1,parms.nr_sets);
        parms.nr_sets*ones(1,parms.nr_sets)];
    nonlcon = @prot2_con2;

    % [x, fval, exitflag, ouput, lambda] = ...
        fmincon(fun,x0,A,b,Aeq,beq,lb,ub,nonlcon,options)


    problem = createOptimProblem('fmincon','objective', fun, 'x0', x0,'Aineq', A,...
         'bineq',b, 'Aeq', Aeq, 'beq', beq,  'lb', lb, 'ub', ub, 'nonlcon', ...
             nonlcon,'options',options);
    % problem.Objective.first = fun;
    % problem.Objective.second = fun2;
    ms = MultiStart( 'UseParallel',true,'StartPointsToRun', 'bounds');
    [x,f,exitflag] = run(ms, problem, 30)
    prot2_params2
    [K_bend,Dtheta,Dy] = K_bend_setfun_prot2_V4(x(1,:),x(2,:),x(3,:),x(4,:),parms)
    [K_ax] = K_ax_setfun_prot2_V2(x(1,:),x(2,:),x(3,:),parms);
    dz = parms.Fz/K_ax
    end
    end
```

Constraint functions:

```
    function [c,ceq] = prot2_con2(x)
% Constraint function:

% Constant parameters !put before design par, otherwise you overide it!


% Design parameters !Uncomment the ones you want to use!
W_flex      = x(1,:);
t_flex      = x(2,:);
L_flex      = x(3,:);
dist_flex   = x(4,:);
parms.nr_sets = x(5);
```

```

prot2_params2;


[K_bend,Dtheta,Dy] = K_bend_setfun_prot2_V4(W_flex,t_flex,L_flex,dist_flex,parms);
c =[];

% % Length constraint for the distance between flexures
% c(1) = (max(dist_flex)+2*max(t_flex))/parms.dist_set-1;

% %constraint to get a deflection desired_Dy
c(1) = parms.desired_Dy_low/Dy-1;
c(2) = Dy/parms.desired_Dy_up-1;

% % Constraints that manage the angle of each of the stages
for i = 2:length(Dtheta)

    c(end+1) = mean(Dtheta(2:end))/(Dtheta(i)+parms.angle_tol)-1;

end
for i = 2:length(Dtheta)

    c(end+1) = (Dtheta(i)-parms.angle_tol)/mean(Dtheta(2:end))-1;

end
ceq = [];
```

Objective function, chose one of the ratio, axial stiffness or bending stiffness

```
function f = prot2_obj2(x)

% Design parameters
W_flex      = x(1,:);
t_flex      = x(2,:);
L_flex      = x(3,:);
dist_flex   = x(4,:);
parms.nr_sets = x(5);

% Other parameters
prot2_params2


% Calculation of objective values
k_bend = K_bend_setfun_prot2_V4(W_flex,t_flex,L_flex,dist_flex,parms);

k_ax = K_ax_setfun_prot2_V2(W_flex,t_flex,L_flex,parms);

stiff_ratio = k_ax/(k_bend);

%objective function
f = k_ax;
```

Bibliography

[1] Mohammad Mehdi Alemi et al. "A passive exoskeleton reduces peak and mean EMG during symmetric and asymmetric lifting". In: *Journal of Electromyography and Kinesiology* 47 (Aug. 2019), pp. 25–34. ISSN: 1050-6411. DOI: 10.1016/J.JELEKIN.2019.05.003.

[2] Larry L. Howell, Spencer P. Magleby, and Brian M. (Brian Mark) Olsen. "Handbook of compliant mechanisms". In: ().

[3] Kirsten Huysamen, Valerie Power, and Leonard O'Sullivan. "Elongation of the surface of the spine during lifting and lowering, and implications for design of an upper body industrial exoskeleton". In: *Applied Ergonomics* 72 (Oct. 2018), pp. 10–16. ISSN: 0003-6870. DOI: 10.1016/J.APERGO.2018.04.011.

[4] Axel S. Koopman et al. "Biomechanical evaluation of a new passive back support exoskeleton". In: *Journal of Biomechanics* 105 (May 2020), p. 109795. ISSN: 0021-9290. DOI: 10.1016/J.JBIOMECH.2020.109795.

[5] *Laevo exoskeleton*. URL: https://www.laevo-exoskeletons.com/flex (visited on 06/30/2022).

[6] Michiel P. de Looze et al. "Exoskeletons for industrial application and their potential effects on physical work load". In: *https://doi.org/10.1080/00140139.2015.1081988* 59.5 (May 2015), pp. 671–681. ISSN: 13665847. DOI: 10.1080/00140139.2015.1081988. URL: https://www.tandfonline.com/doi/abs/10.1080/00140139.2015.1081988.

[7] Robin Mak. "A Curved Compliant Differential Mechanism with Neutral Stability". In: (2021).

[8] Yong Mo Moon. "Bio-mimetic design of finger mechanism with contact aided compliant mechanism". In: *Mechanism and Machine Theory* 42.5 (May 2007), pp. 600–611. ISSN: 0094114X. DOI: 10.1016/j.mechmachtheory.2006.04.014.

[9] Bhivraj Suthar and Seul Jung. "Design and Bending Analysis of a Metamorphic Parallel Twisted-Scissor Mechanism". In: *Journal of Mechanisms and Robotics* 13.4 (Aug. 2021). ISSN: 1942-4302. DOI: 10.1115/1.4050813. URL: http://asmedigitalcollection.asme.org/mechanismsrobotics/article-pdf/13/4/040901/6724391/jmr%7B%5C_%7D13%7B%5C_%7D4%7B%5C_%7D040901.pdf.